Conformational and Structural Studies of Aminomethyl Cyclopropane from Temperature Dependent FT-IR Spectra of Rare Gas Solutions and *ab Initio* Calculations

James R. Durig,* Chao Zheng,† Robin D. Warren, Peter Groner, Charles J. Wurrey, and Todor K. Gounev

Department of Chemistry, University of Missouri-Kansas City, Kansas City, Missouri 64110

Wouter A. Herrebout and Benjamin J. van der Veken

Department of Chemistry, Universitair Centrum Antwerpen, 171 Groenenborgerlaan, Antwerpen 2020 Belgium

Received: April 30, 2003; In Final Form: July 14, 2003

Infrared (3500−50 cm^{-1}) spectra of gaseous and Raman (3500−50 cm^{-1}) spectra of liquid aminomethyl cyclopropane (cyclopropyl methylamine), c−$C_3H_5CH_2NH_2$ have been recorded. Additional variable temperature (−55 to −100 °C) studies of the mid-infrared (3500−400 cm^{-1}) spectra of the sample dissolved in liquid xenon as well as variable temperature (−79 to −112 °C) studies of the far-infrared spectra (600−50 cm^{-1}) of krypton solutions have been obtained. From these data the enthalpy difference has been determined to be 109 ± 11 cm^{-1} (1.30 ± 0.13 kJ/mol) between the most stable gauche−gauche-1 (Gg-1) conformer (the first gauche designation, capital G, for the heavy atom conformation along the C−C bond, and the second gauche designation, lower case g, for the amino torsion along C−N bond) and the second most stable conformation, gauche-trans (Gt). The third most stable conformer is the cis-gauche (Cg) form with an enthalpy difference of 267 ± 28 cm^{-1} (3.19 ± 0.33 kJ/mol) to the most stable conformer. Larger enthalpy values of 400 ± 40 cm^{-1} and 480 ± 48 cm^{-1} were obtained for the Gg-2 and Ct conformers, respectively. From these data, the following conformer percentages are estimated at ambient temperature: 49% Gg-1, 29% Gt, 13% Cg, 7% Gg-2, and 2% Ct. Ab initio calculations have been carried out with several different basis sets up to MP2/6-311G(2df,2pd) as well as with diffuse functions to determine the conformational stability. Without diffuse functions, the Gt conformer is predicted as the most stable conformer, whereas with diffuse functions, the Gg-1 form is predicted to be the most stable rotamer, and the density functional calculations by the B3LYP method with the same corresponding basis sets all predict the Gt form as the most stable conformer. Additionally, force constants, infrared intensities, Raman activities, depolarization ratios, and scaled vibrational frequencies have been determined from MP2/6-31G(d) calculations. Vibrational assignments are provided for most of the fundamentals for the Gg-1 and Gt conformers. Adjusted r_0 structural parameters have been obtained by combining ab initio MP2/6-311+G(d,p) predicted values and previously reported microwave data for the Gg-1 and Gt forms. Many of the determined results are compared to the corresponding parameters for some other similar organoamines.

Introduction

For molecules that contain an asymmetrically substituted halomethyl group bonded to a symmetrical cyclopropane ring, c−$C_3H_5CH_2X$ where X = F, Cl, Br, and I, two staggered conformers of cis and gauche structure are possible, whereas the eclipsed forms have been predicted to be unstable.[1] Initially, there was considerable controversy as to whether more than one conformer was present at room temperature for the chloride from different microwave studies.[2−4] Molecular mechanics calculations in conjunction with electron diffraction experiments led to the conclusion[5] that the gauche conformer is the predominant form with an energy difference between the conformers of 577 cm^{-1} (6.90 kJ/mol). These results were supported[6] by vibrational and ΔH studies from which it was concluded that the relative abundances of the conformers of chloromethyl cyclopropane are 95% gauche and 5% cis in the liquid phase at room temperature. For bromomethyl cyclopropane[7] 98% was in the gauche form and 2% in the cis conformation. More recent variable temperature studies[8] of the infrared spectra of xenon solutions gave enthalpy differences of 274 ± 21 cm^{-1} (3.28 ± 0.25 kJ/mol) and 383 ± 29 cm^{-1} (4.58 ± 0.35 kJ/mol) for the chloride and bromide, respectively, with 12% and 8% of the cis forms present at ambient temperature. These experimental results are consistent with predictions from molecular mechanics calculations.[9] However, molecular mechanics calculations predict the cis conformer of fluoromethyl cyclopropane to be more stable than the gauche form by 189 cm^{-1}. Ab initio MP2/6-311+G(d,p) calculations predicted[8] the same conformer stability for the chloride and bromide but with energy differences of more than 200 cm^{-1} larger than the experimental ΔH values. In contrast, for the fluoromethyl cyclopropane molecule, ab initio calculations predict the gauche conformer more stable by 70 cm^{-1}, but it has been reported[10] that this molecules is so unstable that its conformational stability has not been measured.

* Corresponding author. Phone: 01 816-235-6038. Fax: 01 816-235-2290. E-mail: durigj@umkc.edu.

† Taken in part from the thesis of C. Zheng, which will be submitted to the Department of Chemistry of the University of Missouri-Kansas City, Kansas City, MO in partial fulfillment of the Ph.D. degree.

10.1021/jp030552e CCC: $25.00
Published on Web 08/26/2003

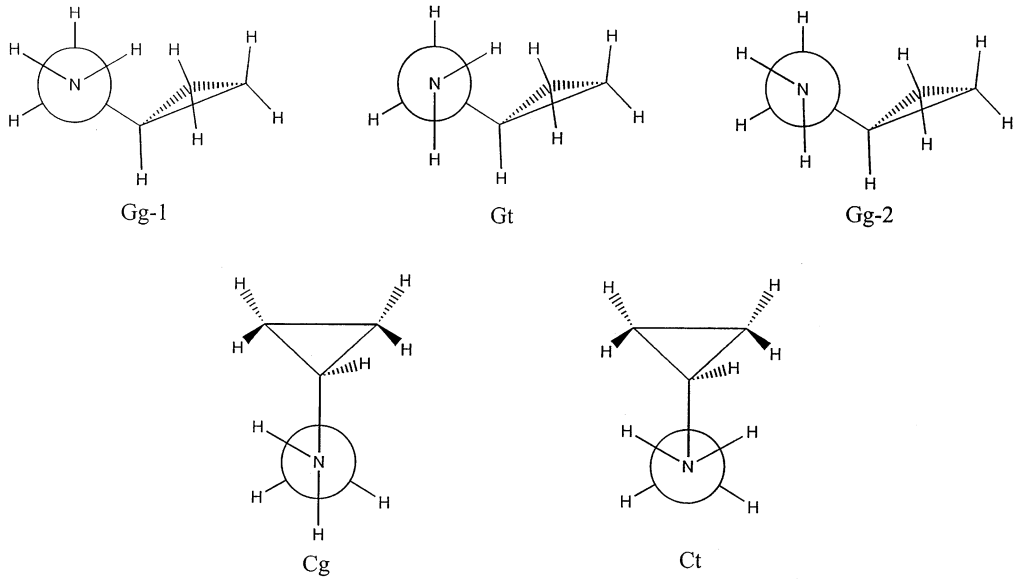

Figure 1. The five possible conformers of aminomethyl cyclopropane where the capital letters C (Cis) and G (Gauche) indicate the relative position of the amino group to the three-membered ring and the second letter (lower case) t (trans), g-1 (gauche-*1*) or g-2 (gauche-*2*) the relative position of the amino rotor.

When the halogen atom is replaced with either the ethynyl,[11,12] $-C\equiv C-H$, or the isoelectric cyano group,[13] $-C\equiv N$, the results are quite different; ab initio calculations predict the cis conformer to be the more stable form for both molecules. The cis conformer of ethynylmethyl cyclopropane was determined[11] to be more stable than the gauche form with a ΔH value of 147 ± 14 cm^{-1} (1.76 ± 0.17 kJ/mol). This value is consistent with the ab initio MP2/6-311+G(2d,2p) predicted energy difference of 174 cm^{-1} (2.08 kJ/mol). A similar energy difference[13] of 134 cm^{-1} was predicted for cyanomethyl cyclopropane utilizing the same basis set and level. However, the gauche conformer of cyanomethyl cyclopropane proved to be more stable[13] by 54 ± 4 cm^{-1} (0.65 ± 0.05 kJ/mol) according to variable temperature studies of the infrared spectra of xenon solutions. Therefore, it does not appear that ab initio predictions for the conformational stabilities of these monosubstituted methylcyclopropanes are reliable when the energy differences are less than 200 cm^{-1}.

As a continuation of our conformational stability studies of methylcyclopropanes, we have turned our attention to aminomethyl cyclopropane, $c-C_3H_5CH_2NH_2$. This molecule provides an additional challenge because we have found that the addition of diffuse functions to the basis set for both ethylamine[14] and allylfluoride[15] change the ab initio predicted stability from the correct trans and cis conformations, respectively, to the gauche rotamers. Finally, it should be noted that there are five potential conformers for aminomethyl cyclopropane and they are shown in Figure 1.

The infrared and Raman spectra of aminomethyl cyclopropane have been recorded of the gas and/or liquid and solid. Additionally, variable temperature mid-infrared spectra have been recorded of the sample dissolved in liquid xenon and similar spectra from 600 to 50 cm^{-1} have been recorded of the sample dissolved in liquid krypton. Ab initio calculations[16] have been carried out utilizing the 6-31G(d) basis set at the restricted Hartree−Fock (RHF) level and with full electron correlation by the perturbation method[17] to the second order (MP2) as well as density functional theory (DFT) calculations by the B3LYP method. From these calculations, force constants, vibrational frequencies, infrared and Raman intensities, depolarization ratios, structural parameters, and conformational stabilities have been obtained. Structural parameters and conformational stabilities have been calculated with several larger basis sets. From the ab initio MP2(full)/6-311+G(d,p) predictions and previously reported[18] microwave rotational constants for two conformers, adjusted r_0 parameters were obtained for these conformers. The results of these vibrational spectroscopic, structural, and theoretical studies are reported herein.

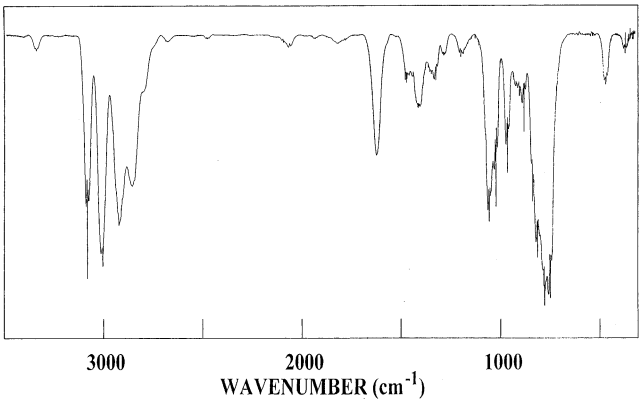

Figure 2. Mid-infrared spectrum of aminomethyl cyclopropane gas at room temperature.

Experimental Section

The sample of aminomethyl cyclopropane was purchased from Aldrich Chemical Co., Milwaukee, WI, with a stated purity of 99%. The sample was further purified by means of a low-pressure low-temperature fractionation column and the purity of the sample was checked by mass and NMR spectra. The sample was kept in the dark at low temperature until it was used.

The mid-infrared spectrum of the gas (Figure 2) was obtained from 3500 to 400 cm^{-1} on a Perkin-Elmer model 2000 Fourier transform spectrophotometer equipped with a Ge/CsI beam splitter and a DTGS detector. Atmospheric water vapor was removed from the spectrophotometer housing by purging with dry nitrogen gas. The spectrum of the gas was obtained with the sample contained in a 10-cm cell fitted with CsI windows.

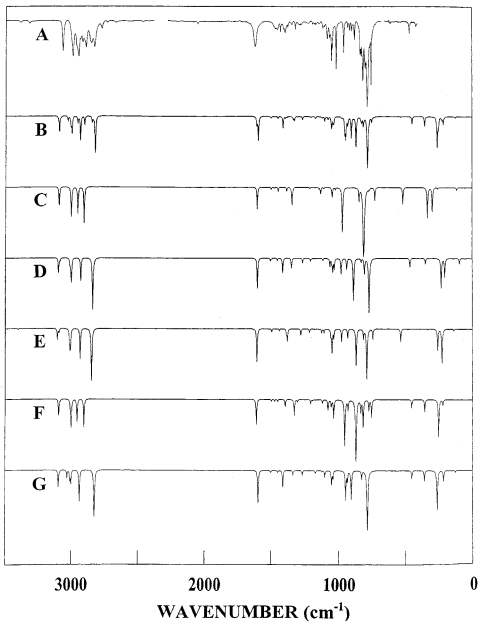

Figure 3. Mid-infrared spectra of aminomethyl cyclopropane: (A) xenon solution at −75 °C; (B) simulated spectrum of a mixture of the five conformers with ΔH of 109 cm^{-1} for Gt, ΔH of 267 cm^{-1} for Cg, ΔH of 400 cm^{-1} for Gg-2, and ΔH of 448 cm^{-1} for Ct relative to the most stable Gg-1 form; (C) calculated spectrum for pure Ct; (D) calculated spectrum for pure Gg-2; (E) calculated spectrum for pure Cg; (F) calculated spectrum for pure Gt; and (G) calculated spectrum for pure Gg-1.

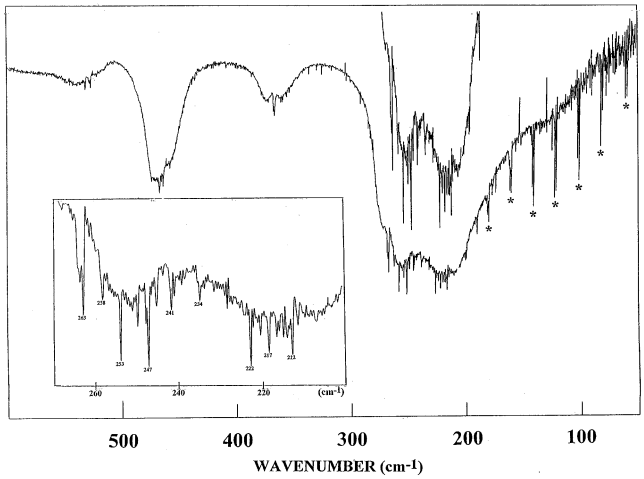

Figure 4. Far-infrared spectrum of aminomethyl cyclopropane gas at room temperature. Bands labeled with asterisks are due to ammonia.

The theoretical resolution used to obtain the spectra of both the gas and solid was 1.0 cm^{-1}, usually, 100 interferograms were collected and averaged and the data were transformed with a boxcar truncation function.

The mid-infrared spectra of the sample dissolved in liquefied xenon (Figure 3) as a function of temperature were recorded on a Bruker model IFS 66 Fourier transform spectrometer equipped with a Globar source, a Ge/KBr beam splitter and a DTGS detector. In all cases, 100 interferograms were collected at 1.0 cm^{-1} resolution, averaged, and transformed with a boxcar truncation function. For these studies, a specially designed cryostat cell[13] was used.

The far-infrared spectrum of the gas (Figure 4) was recorded on the Perkin-Elmer model 2000 spectrometer equipped with a metal grid beam splitter and a DTGS detector. The spectrum was recorded with the sample contained in a 12-cm cell

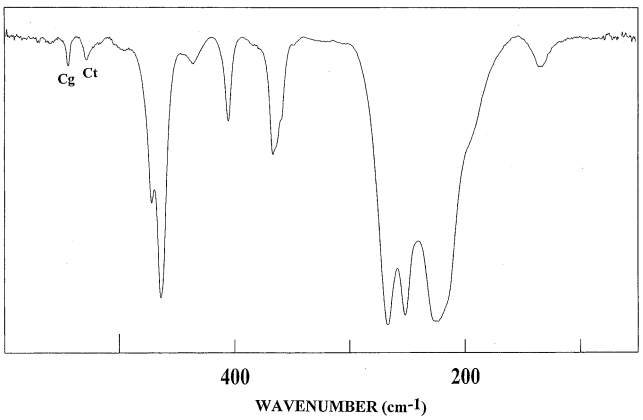

Figure 5. Far-infrared spectrum of aminomethyl cyclopropane in liquid krypton at −115 °C.

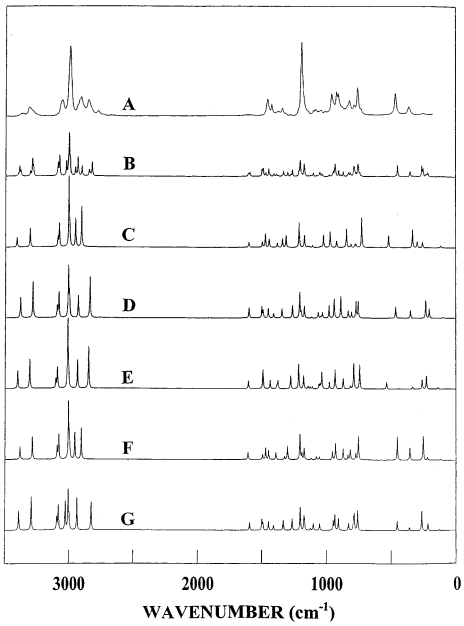

Figure 6. Raman spectra of aminomethyl cyclopropane: (A) liquid at room temperature; (B) simulated spectrum of a mixture of the five conformers with ΔH of 109 cm^{-1} for Gt, ΔH of 267 cm^{-1} for Cg, ΔH of 400 cm^{-1} for Gg-2, and ΔH of 448 cm^{-1} for Ct relative to the most stable Gg-1 form; (C) calculated spectrum for pure Ct; (D) calculated spectrum for pure Gg-2; (E) calculated spectrum for pure Cg; (F) calculated spectrum for pure Gt; (G) calculated spectrum for pure Gg-1.

equipped with polyethylene windows, 0.5 cm^{-1} resolution and with 256 scans averaged to give a satisfactory signal-to-noise ratio.

The far-infrared spectra of the sample dissolved in liquid krypton were recorded on a Bruker model IFS 66 v/S Fourier transform spectrophotometer equipped with a Globar source, a 6.0-μm Mylar beam splitter, and a liquid helium cooled Si bolometer. The sample was contained in a 7-cm cell fitted with Si windows and the sample added as described for the mid-infrared studies. For all spectra, 250 interferograms were collected at 0.5-cm^{-1} resolution, averaged and transformed with a Blackman-Harris three-term function. Typical spectra are shown in Figure 5.

The Raman spectra were recorded with a Spex model 1403 spectrophotometer equipped with a Spectra-Physics model 164 argon ion laser operating on the 5145 Å line. The laser power used was 0.5 W with instrument resolution of 3 cm^{-1}. The spectra of the liquid and solid were recorded with the sample

TABLE 1: Observed and Calculated Frequencies (cm^{-1}) for *Gg-1* Aminomethyl Cyclopropane

vib no.	fundamental	ab initio[a]	fix scaled[b]	IR int.[c]	Raman act.[d]	dp ratio	IR gas	IR Kr[e]	Raman liquid	PED[f]	A[g]	B[g]	C[g]
ν_1	NH_2 antisymmetric stretch	3613	3389	0.1	67.0	0.70	3405	3396	3375	$100S_1$	5	81	14
ν_2	NH_2 symmetric stretch	3509	3292	0.7	111.4	0.13	3344	3326	3319	$100S_2$	92	4	4
ν_3	rCH_2 antisymmetric stretch	3300	3096	16.4	36.5	0.56	3088	3078	3075	$96S_3$	22	4	74
ν_4	rCH_2 antisymmetric stretch	3288	3084	0.7	74.0	0.74			3065	$96S_4$	10	49	41
ν_5	CH stretch	3230	3030	6.7	81.4	0.25				$98S_5$	3	1	96
ν_6	rCH_2 symmetric stretch	3206	3008	8.5	110.2	0.07	3009	3002	3001	$81S_6$, $18S_7$	63	12	25
ν_7	rCH_2 symmetric stretch	3198	3000	12.3	38.3	0.27	3013	3002	3001	$81S_7$, $17S_6$	1	89	10
ν_8	CH_2 antisymmetric stretch	3131	2937	35.3	88.0	0.40	2927	2927	2915	$68S_8$, $32S_9$	14	71	15
ν_9	CH_2 symmetric stretch	3012	2825	65.7	72.3	0.17	2847	2839	2859	$68S_9$, $32S_8$	7	17	76
ν_{10}	NH_2 deformation	1715	1591	36.7	8.3	0.71	1619	1615	1618	$78S_{10}$, $21S_{30}$	25	34	41
ν_{11}	CH_2 deformation	1579	1498	2.2	10.4	0.74	1476	1479	1459	$58S_{11}$, $32S_{12}$	20	16	64
ν_{12}	rCH_2 deformation	1570	1490	0.2	7.0	0.67	1466	1463	1459	$43S_{12}$, $40S_{11}$, $11S_{17}$	89	4	7
ν_{13}	rCH_2 deformation	1525	1447	2.0	8.3	0.75	1434	1428	1427	$99S_{13}$	21	79	0
ν_{14}	CH_2 wag	1493	1408	16.1	4.4	0.63	1401	1393	1404	$37S_{14}$, $16S_{15}$, $15S_{18}$, $11S_{12}$	91	5	4
ν_{15}	CH in-plane bend	1423	1334	4.3	8.7	0.60	1352	1346	1353	$23S_{15}$, $26S_{14}$, $15S_{16}$, $15S_{21}$	94	4	2
ν_{16}	CH_2 twist	1350	1266	4.1	9.0	0.58	1271	1279	1278	$41S_{16}$, $21S_{14}$, $12S_{21}$	74	25	1
ν_{17}	ring breathing	1271	1203	0.1	17.0	0.23	1195	1192	1193	$42S_{17}$, $20S_{15}$, $12S_{31}$	57	23	20
ν_{18}	CC stretch	1255	1174	2.1	5.8	0.53			1170	$14S_{18}$, $19S_{25}$, $15S_{15}$, $14S_{21}$	7	0	93
ν_{19}	rCH_2 twist	1237	1170	0.9	8.4	0.71			1170	$38S_{19}$, $46S_{28}$, $14S_{20}$	9	74	17
ν_{20}	CH out-of-plane bend	1178	1102	1.0	1.4	0.46	1103	1103	1103	$55S_{20}$, $37S_{18}$	4	49	47
ν_{21}	NH_2 twist	1214	1124	6.0	4.6	0.12	1122	1115	1118	$19S_{21}$, $23S_{16}$	3	0	97
ν_{22}	CN stretch	1112	1053	12.4	4.1	0.63	1054	1050	1047	$67S_{22}$	80	20	0
ν_{23}	rCH_2 wag	1109	1050	2.5	0.1	0.74	1053		1047	$87S_{23}$	19	72	9
ν_{24}	rCH_2 wag	1100	1041	7.3	0.2	0.71	1046	1044	1047	$82S_{24}$	73	2	25
ν_{25}	CH_2 rock	1023	946	32.1	4.9	0.58	959	959	962	$20S_{25}$, $20S_{26}$, $12S_{21}$, $11S_{18}$	53	1	46
ν_{26}	ring deformation	991	933	8.9	8.6	0.50	929	928	924	$24S_{26}$, $20S_{27}$	0	93	7
ν_{27}	ring deformation	967	905	31.7	6.1	0.62	908	913	911	$33S_{27}$, $14S_{30}$	22	3	75
ν_{28}	rCH_2 rock	870	826	7.5	3.4	0.73	827	826	823	$28S_{28}$, $18S_{27}$, $15S_{19}$, $15S_{20}$	13	15	72
ν_{29}	rCH_2 rock	833	789	2.5	4.9	0.54	799	795		$29S_{29}$, $19S_{26}$, $10S_{18}$	15	0	85
ν_{30}	NH_2 wag	895	783	114.1	6.5	0.74	777	781	788	$41S_{30}$, $20S_{25}$, $16S_{27}$	36	24	40
ν_{31}	rCH_2 twist	801	757	0.2	8.4	0.60	758	761	760	$39S_{31}$, $24S_{29}$, $16S_{26}$, $12S_{18}$	1	99	0
ν_{32}	CCN bend	476	451	7.5	2.1	0.48	464	464	466	$44S_{32}$, $25S_{35}$	77	5	18
ν_{33}	ring-C in-plane bend	382	358	9.9	0.5	0.17	365	366	369	$60S_{33}$, $21S_{34}$	84	14	2
ν_{34}	NH_2 torsion	295	265	48.8	1.9	0.68	263	266		$59S_{34}$, $23S_{33}$	70	30	0
ν_{35}	ring-C out-of-plane bend	234	218	9.6	0.5	0.72	222	226	250	$46S_{35}$, $30S_{32}$, $16S_{34}$	19	81	0
ν_{36}	asymmetric torsion	127	127	1.9	0.1	0.50	129	135		$90S_{36}$	29	71	0

[a] MP2/6-31G(d) predicted values. [b] MP2/6-31G(d) fixed scaled frequencies with factors of 0.88 for CH and NH stretches, 0.70 for CNH bends, 0.75 for amino torsion, 1.0 for asymmetric torsion, and 0.90 for all other modes. [c] Calculated infrared intensities in km/mol from MP2/6-31G(d). [d] Calculated Raman activities in $Å^4$/amu from MP2/6-31G(d). [e] Frequencies from Kr solution at −110 °C. [f] Calculated with MP2/6-31G(d), and contributions of less than 10% are omitted. [g] *A, B,* and *C* values in the last three columns are percentage infrared band contours.

contained in sealed capillaries, and a typical Raman spectrum is shown in Figure 6. The wavenumbers for all of the observed fundamentals for all five conformers are listed in Tables 1−5 in all of the physical states.

Ab Initio Calculations. The LCAO-MO-SCF restricted Hartree−Fock calculations were performed with the Gaussian-98 program[16] using Gaussian-type basis functions. The energy minima with respect to the nuclear coordinates were obtained by the simultaneous relaxation of all the geometric parameters using the gradient method of Pulay.[19] Calculations were also carried out with full electron correlation by the perturbation method[17] to second order up to the 6-311+G(2df,2pd) basis set. Density functional theory (DFT) calculations made with the Gaussian 98 program[16] were restricted to the hybrid B3LYP method. The determined energy differences that resulted from these various calculations are listed in Table 6.

To obtain a complete description of the molecular motions involved in the normal modes of aminomethyl cyclopropane, a normal coordinate analysis has been carried out. It has been shown from our past studies of a series of amine and cyclopropyl molecules that properly scaled MP2/6-31G(d) frequencies have an average error of less than 1% (less than 0.8% for bending and torsional modes). We have also found that a larger basis set does little to improve vibrational frequency predictions. Thus, the force field in Cartesian coordinates was obtained with the Gaussian 98 program[16] from the MP2/6-31G(d) level of calculation. The internal coordinates shown in Figure 7 were used to form the symmetry coordinates listed in Table 1S. The B-matrix elements[20] were used to convert the ab initio force field from Cartesian coordinates into the force field in desired internal coordinates. These force constants were used to reproduce the ab initio vibrational frequencies for conformers that are given in Tables 1−5. The diagonal elements of the force field in internal coordinates were then multiplied by scaling factors of 0.88 for the CH and NH stretches, 0.70 for CNH bends, 0.75 for the amino torsion, 1.0 for the asymmetric torsion, and 0.90 for all other modes. The geometrical average of the scaling factors was applied to the off-diagonal force constants. The calculation was repeated to obtain the fixed scaled force field, scaled vibrational frequencies, and potential energy distributions (PED) given in Tables 1−5.

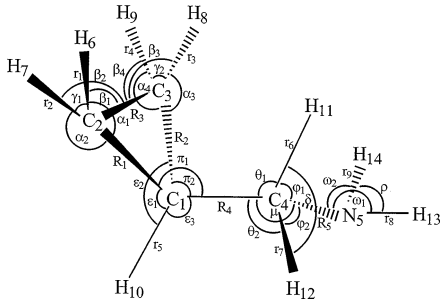

Figure 7. Internal coordinates of aminomethyl cyclopropane.

The infrared and Raman spectra were simulated as shown in Figures 3 and 6, respectively. The frequencies, Raman scattering activities, and infrared intensities were obtained from the output of the ab initio calculations. The Raman scattering cross sections, $\partial\sigma_j/\partial\Omega$, which are proportional to the Raman intensities, can

TABLE 2: Observed and Calculated Frequencies (cm^{-1}) for *Gt* Aminomethyl Cyclopropane

vib no.	fundamental	ab initio[a]	fix scaled[b]	IR int.[c]	Raman act.[d]	dp ratio	IR gas	IR Kr[e]	Raman liquid	PED[f]	*A*[g]	*B*[g]	*C*[g]
ν_1	NH_2 antisymmetric stretch	3603	3380	0.1	44.9	0.74		3388	3375	$100S_1$	39	33	28
ν_2	NH_2 symmetric stretch	3502	3285	0.2	75.1	0.11		3326	3319	$100S_2$	0	89	11
ν_3	rCH_2 antisymmetric stretch	3299	3095	15.2	37.8	0.62	3087	3078	3075	$94S_3$	25	3	72
ν_4	rCH_2 antisymmetric stretch	3286	3083	1.2	72.2	0.74			3065	$94S_4$	11	41	48
ν_5	CH stretch	3199	3001	17.4	42.0	0.43	3009	3002	3001	$73S_5$, $23S_7$	18	7	75
ν_6	rCH_2 symmetric stretch	3206	3008	4.7	156.2	0.06	3009	3002	3001	$73S_6$, $16S_7$, $11S_5$	76	24	0
ν_7	rCH_2 symmetric stretch	3197	2999	16.0	26.8	0.32	3009	3002	3001	$61S_7$, $25S_6$, $13S_5$	1	61	38
ν_8	CH_2 antisymmetric stretch	3151	2956	23.7	73.6	0.70		2958	2926	$95S_8$	16	52	32
ν_9	CH_2 symmetric stretch	3095	2904	30.0	84.1	0.07		2902	2897	$98S_9$	0	62	38
ν_{10}	NH_2 deformation	1727	1604	26.2	8.0	0.72	1622	1618	1618	$78S_{10}$, $21S_{30}$	0	67	33
ν_{11}	CH_2 deformation	1550	1470	1.7	11.5	0.75	1455	1450	1449	$91S_{11}$	6	17	77
ν_{12}	rCH_2 deformation	1573	1493	1.6	4.9	0.75	1469	1476	1459	$74S_{12}$, $15S_{17}$	11	1	88
ν_{13}	rCH_2 deformation	1526	1447	2.2	8.6	0.75	1434	1428	1427	$98S_{13}$	19	80	1
ν_{14}	CH_2 wag	1390	1302	15.3	2.6	0.71	1322	1319	1320	$76S_{14}$, $10S_{15}$	98	0	2
ν_{15}	CH in-plane bend	1465	1390	6.2	6.2	0.43	1375	1372	1384	$36S_{15}$, $16S_{14}$, $13S_{12}$, $12S_{18}$, $11S_{17}$	93	3	4
ν_{16}	CH_2 twist	1429	1325	2.4	11.2	0.75	1345	1342	1345	$46S_{16}$, $40S_{21}$	74	0	26
ν_{17}	ring breathing	1266	1206	3.9	18.9	0.21	1195	1192	1193	$48S_{17}$, $28S_{15}$	95	4	1
ν_{18}	CC stretch	1127	1055	5.0	1.8	0.68			1047	$14S_{18}$, $30S_{22}$, $11S_{16}$, $10S_{21}$, $10S_{15}$	58	38	4
ν_{19}	rCH_2 twist	1237	1173	0.5	8.2	0.75			1170	$39S_{19}$, $47S_{28}$, $13S_{20}$	8	74	18
ν_{20}	CH out-of-plane bend	1182	1119	3.4	1.2	0.63			1118	$58S_{20}$, $26S_{19}$	68	22	10
ν_{21}	NH_2 twist	1287	1191	0.9	4.7	0.48			1193	$13S_{21}$, $23S_{31}$, $15S_{16}$, $13S_{25}$, $10S_{33}$	35	44	21
ν_{22}	CN stretch	1160	1078	9.4	2.1	0.54	1085	1082	1089	$35S_{22}$, $14S_{30}$	54	5	41
ν_{23}	rCH_2 wag	1109	1052	2.1	0.1	0.65			1047	$97S_{23}$	3	97	0
ν_{24}	rCH_2 wag	1097	1036	18.3	0.2	0.73	1019	1015	1015	$88S_{24}$	81	1	18
ν_{25}	CH_2 rock	901	832	11.4	2.2	0.44	835	834	835	$36S_{25}$, $25S_{29}$	100	0	0
ν_{26}	ring deformation	1026	953	63.2	4.5	0.57	962	959	962	$16S_{26}$, $13S_{18}$, $12S_{31}$	100	0	0
ν_{27}	ring deformation	981	929	8.9	8.8	0.57	927		924	$40S_{27}$, $27S_{26}$	1	79	20
ν_{28}	rCH_2 rock	868	814	28.5	4.6	0.74	812	812	812	$31S_{28}$, $22S_{27}$, $18S_{20}$, $16S_{19}$	66	33	1
ν_{29}	rCH_2 rock	820	772	10.3	2.8	0.51				$30S_{29}$, $19S_{25}$, $14S_{31}$, $11S_{26}$	93	2	5
ν_{30}	NH_2 wag	959	869	119.6	5.5	0.48	877	876	884	$37S_{30}$, $14S_{24}$, $13S_{27}$, $10S_{10}$, $10S_{26}$	91	1	8
ν_{31}	rCH_2 twist	800	752	17.1	9.7	0.54	748	750	753	$32S_{31}$, $19S_{26}$, $16S_{29}$, $15S_{18}$	94	4	2
ν_{32}	CCN bend	479	452	7.3	4.9	0.52	461	464	466	$41S_{32}$, $27S_{35}$	38	59	3
ν_{33}	ring-C in-plane bend	382	356	11.3	1.9	0.38	366	366	364	$55S_{33}$, $28S_{34}$	10	42	48
ν_{34}	NH_2 torsion	286	255	44.6	2.2	0.73	247	251		$64S_{34}$, $28S_{33}$	13	24	63
ν_{35}	ring-C out-of-plane bend	236	222	5.0	0.2	0.65	218	221	250	$56S_{35}$, $33S_{32}$	6	76	18
ν_{36}	asymmetric torsion	122	122	0.4	0.1	0.38	125	132		$92S_{36}$	60	4	36

[a] MP2/6-31G(d) predicted values. [b] MP2/6-31G(d) fixed scaled frequencies with factors of 0.88 for CH and NH stretches, 0.70 for CNH bends, 0.75 for amino torsion, 1.0 for asymmetric torsion, and 0.90 for all other modes. [c] Calculated infrared intensities in km/mol from MP2/6-31G(d). [d] Calculated Raman activities in $Å^4$/amu from MP2/6-31G(d). [e] Frequencies from Kr solution at −110 °C. [f] Calculated with MP2/6-31G(d), and contributions of less than 10% are omitted. [g] *A*, *B*, and *C* values in the last three columns are percentage infrared band contours.

be calculated from the scattering activities and the predicted frequencies for each normal mode.[21−24] To obtain the polarized Raman cross sections, the polarizabilities are incorporated into S_j by multiplying it by $(1-\rho_j)/(1+\rho_j)$, where ρ_j is the depolarization ratio of the *j*th normal mode. The Raman scattering cross sections and the predicted scaled frequencies were used together with a Lorentzian line-shape function to obtain the calculated spectra.

The predicted Raman spectra of the pure Gg-1, Gt, Cg, Gg-2 and Ct conformers of $c-C_3H_5CH_2NH_2$ are shown in Figure 6G, 6F, 6E, 6D, 6C, respectively. The predicted Raman spectrum of the mixture of the five conformers, with relative concentrations calculated for all equilibrium mixture at 25 °C using the experimentally determined enthalpy differences, is shown in Figure 6B. This spectrum should be compared with the experimental Raman spectrum of the liquid at room temperature shown in Figure 6A. It is clear that the simulated Raman spectrum closely resembles the observed spectrum. Although there are some differences between calculated and experimental intensities, these data demonstrate the utility of ab initio calculations in predicting the spectrum for conformer identification and vibrational assignments for these types of substituted methylcyclopropane molecules. It should be noted that some of the differences may be the result of hydrogen bonding in the liquid.

The infrared spectra were also predicted from the MP2/6-31G(d) calculations. Infrared intensities were calculated based on the dipole moment derivatives with respect to the Cartesian coordinates. The derivatives were taken from the ab initio calculations transformed to normal coordinates by

$$\left(\frac{\partial \mu_u}{\partial Q_i}\right) = \sum_j \left(\frac{\partial \mu_u}{\partial X_j}\right) L_{ij}$$

where Q_i is the *i*th normal coordinate, X_j is the j^{th} Cartesian displacement coordinate, and L_{ij} are elements of transformation matrix between the Cartesian displacement coordinates and normal coordinates. The infrared intensities were then calculated by

$$I_i = \frac{N\pi}{3c^2}\left[\left(\frac{\partial \mu_x}{\partial Q_i}\right)^2 + \left(\frac{\partial \mu_y}{\partial Q_i}\right)^2 + \left(\frac{\partial \mu_z}{\partial Q_i}\right)^2\right]$$

The predicted infrared spectra of the pure Gg-1, Gt, Cg, Gg-2 and Ct conformers are shown in Figure 3, parts G, F, E, D, and C, respectively. The mixture of the five conformers is shown in Figure 3B. These spectra can be compared to the experimental spectra of the sample dissolved in liquefied xenon at −75 °C shown in Figure 3A. Although there are some apparent differ-

TABLE 3: Observed and Calculated Frequencies (cm^{-1}) for *Cg* Aminomethyl Cyclopropane

vib no.	fundamental	ab initio[a]	fix scaled[b]	IR int.[c]	Raman act.[d]	dp ratio	IR gas	IR Kr[e]	Raman liquid	PED[f]	*A*[g]	*B*[g]	*C*[g]
ν_1	NH_2 antisymmetric stretch	3624	3400	1.2	63.7	0.70		3408		$100S_1$	12	7	81
ν_2	NH_2 symmetric stretch	3526	3307	0.1	99.0	0.12				$100S_2$	68	22	10
ν_3	rCH_2 antisymmetric stretch	3312	3107	10.1	28.0	0.74				$89S_3$	69	31	0
ν_4	rCH_2 antisymmetric stretch	3299	3095	3.4	62.1	0.75				$89S_4$, $10S_3$	54	32	14
ν_5	CH stretch	3205	3007	15.2	35.7	0.74				$79S_5$, $20S_6$	1	94	5
ν_6	rCH_2 symmetric stretch	3215	3016	8.3	190.7	0.06				$79S_6$, $20S_5$	89	7	4
ν_7	rCH_2 symmetric tretch	3209	3011	14.8	24.9	0.75				$99S_7$	2	14	84
ν_8	CH_2 antisymmetric stretch	3129	2935	32.9	78.3	0.48				$74S_8$, $26S_9$	6	19	75
ν_9	CH_2 symmetric stretch	3036	2848	79.3	107.9	0.21	2860	2862	2859	$74S_9$, $26S_8$	20	49	31
ν_{10}	NH_2 deformation	1724	1601	37.7	8.3	0.64				$78S_{10}$, $21S_{30}$	55	20	25
ν_{11}	CH_2 deformation	1571	1490	0.9	14.1	0.69				$94S_{11}$	61	8	31
ν_{12}	rCH_2 deformation	1572	1491	2.1	4.8	0.73				$67S_{12}$, $19S_{17}$	74	24	2
ν_{13}	rCH_2 deformation	1513	1435	1.9	7.7	0.74				$100S_{13}$	2	2	96
ν_{14}	CH_2 wag	1466	1382	11.0	6.7	0.72		1393		$41S_{14}$, $17S_{18}$, $15S_{21}$	99	0	1
ν_{15}	CH in-plane bend	1456	1375	4.3	3.5	0.49	1375	1373		$33S_{15}$, $33S_{14}$, $20S_{12}$	86	10	4
ν_{16}	CH_2 twist	1376	1278	5.7	10.2	0.71	1280	1290		$57S_{16}$, $21S_{21}$	60	13	27
ν_{17}	ring breathing	1281	1215	3.3	18.6	0.21				$45S_{17}$, $28S_{15}$	90	3	7
ν_{18}	CC stretch	787	742	9.3	9.8	0.50				$33S_{18}$, $38S_{26}$, $18S_{31}$	1	88	11
ν_{19}	rCH_2 twist	1240	1177	0.7	9.3	0.75				$44S_{19}$, $44S_{28}$, $11S_{20}$	7	3	90
ν_{20}	CH out-of-plane bend	1186	1126	3.5	1.3	0.67				$34S_{20}$, $18S_{19}$	2	33	65
ν_{21}	NH_2 twist	1248	1142	0.4	1.9	0.56	1141	1144		$30S_{21}$, $29S_{16}$, $13S_{25}$	2	14	84
ν_{22}	CN stretch	1176	1108	3.5	1.5	0.74	1106			$10S_{22}$, $24S_{20}$, $16S_{19}$	3	86	11
ν_{23}	rCH_2 wag	1118	1058	5.9	2.5	0.46	1065	1065		$76S_{23}$	50	48	2
ν_{24}	rCH_2 wag	1101	1049	24.0	2.9	0.71				$66S_{24}$, $15S_{22}$	49	38	13
ν_{25}	CH_2 rock	1045	977	11.6	4.0	0.36	992			$23S_{25}$, $21S_{22}$, $13S_{21}$	1	83	16
ν_{26}	ring deformation	1009	932	8.2	10.3	0.43				$39S_{26}$, $17S_{18}$, $14S_{22}$	33	65	2
ν_{27}	ring deformation	897	868	42.7	5.1	0.67	880	878		$37S_{27}$, $23S_{30}$, $17S_{25}$	0	95	5
ν_{28}	rCH_2 rock	845	812	8.3	1.3	0.75				$39S_{28}$, $21S_{20}$, $17S_{19}$, $17S_{25}$	3	32	65
ν_{29}	rCH_2 rock	827	788	0.6	1.0	0.14				$67S_{29}$, $18S_{31}$	55	40	5
ν_{30}	NH_2 wag	934	784	73.0	10.7	0.70	781	777		$32S_{30}$, $45S_{27}$	0	44	56
ν_{31}	rCH_2 twist	1110	1036	8.2	10.3	0.43				$8S_{31}$, $24S_{24}$, $16S_{23}$	33	65	2
ν_{32}	CCN bend	567	535	11.6	1.9	0.66	545	545		$45S_{32}$, $31S_{33}$	19	49	32
ν_{33}	ring-C in-plane bend	256	229	39.6	1.0	0.67	241	241		$34S_{33}$, $47S_{34}$, $14S_{32}$	57	0	43
ν_{34}	NH_2 torsion	284	262	21.2	0.9	0.70	254	258		$47S_{34}$, $23S_{33}$, $27S_{32}$	46	10	44
ν_{35}	ring-C out-of-plane bend	353	335	0.8	0.3	0.74	328	327	334	$85S_{35}$	86	8	6
ν_{36}	asymmetric torsion	139	139	1.7	0.1	0.73	146	145		$98S_{36}$	1	64	35

[a] MP2/6-31G(d) predicted values. [b] MP2/6-31G(d) fixed scaled frequencies with factors of 0.88 for CH and NH stretches, 0.70 for CNH bends, 0.75 for amino torsion, 1.0 for asymmetric torsion, and 0.90 for all other modes. [c] Calculated infrared intensities in km/mol from MP2/6-31G(d). [d] Calculated Raman activities in $Å^4$/amu from MP2/6-31G(d). [e] Frequencies from Kr solution at −110 °C. [f] Calculated with MP2/6-31G(d), and contributions of less than 10% are omitted. [g] *A*, *B*, and *C* values in the last three columns are percentage infrared band contours.

ences between calculated and experimental intensities, e.g. the bands at 750 (ν_{31} rCH_2 twist), 812 (ν_{28} rCH_2 rock) and 1015 cm^{-1} (ν_{24} rCH_2 wag) for the Gt form are much stronger than predicted, and ν_9 at 2839 cm^{-1}, for the Gg-1 form is much weaker than predicted, as a whole. The simulated infrared spectrum closely resembles the observed spectrum, which provides excellent evidence for the quality of the ab initio calculations. It should be noted that some of the differences might be the result of association with the solvent xenon atoms.

Vibrational Assignment. To determine the conformational stabilities of the different forms of aminomethyl cyclopropane, it is necessary to assign bands to each one of the rotamers. However, it is a daunting task to provide a vibrational assignment, because the two major conformers have large abundance at ambient temperature, whereas the other three much less abundant conformers may also have similar abundances to each other.[18] Additionally, the NH_2 modes experience large shifts of their fundamental frequencies in going from the gas to the solid state, particularly the torsion and the rock. Shifts were observed to a lesser extent also by going from the gas to the liquid. Nevertheless, by using the ab initio predicted frequencies, the observed and predicted infrared gas phase band contours, and the band intensities from the infrared and Raman spectra, it has been possible to provide a reasonably complete vibrational assignment for the two major conformers. Additionally, some of the fundamentals have been identified for the other three conformers. Because the rotation of the NH_2 group has little effect on the moments of inertia of aminomethyl cyclopropane, the predicted infrared band contours only differ between those for the two cis conformers (Cg and Ct) and those for the three gauche forms (Gg-1, Gt, and Gg-2). The two different sets of contours are shown in Figure 8, where the major differences are the predicted sub-band structure on the B-type band for the gauche conformers. Because only the Ct conformer

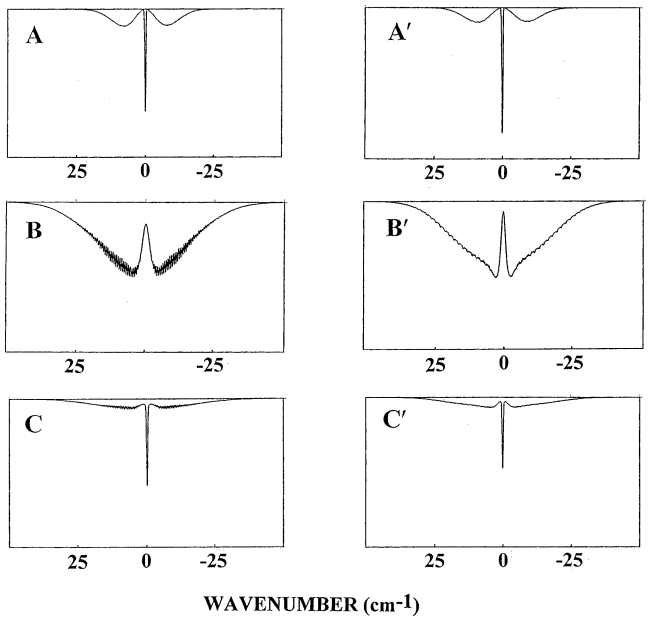

Figure 8. Predicted pure A-, B-, and C-type infrared contours for the Gg-1, Gt, and Gg-2 conformers and pure A′-, B′-, and C′-type contours for the Cg and Ct conformers for aminomethyl cyclopropane.

TABLE 4: Observed and Calculated Frequencies (cm^{-1}) for *Gg-2* Aminomethyl Cyclopropane

vib no.	fundamental	ab initio[a]	fix scaled[b]	IR int.[c]	Raman act.[d]	dp ratio	IR gas	IR Kr[e]	PED[f]	*A*[g]	*B*[g]	*C*[g]
ν_1	NH_2 antisymmetric stretch	3603	3380	0.2	71.9	0.72			$100S_1$	66	3	31
ν_2	NH_2 symmetric stretch	3501	3285	0.7	119.2	0.13			$100S_2$	93	3	4
ν_3	rCH_2 antisymmetric stretch	3304	3099	14.0	33.8	0.68			$92S_3$	24	8	68
ν_4	rCH_2 antisymmetric stretch	3290	3087	2.3	73.8	0.74			$92S_4$	29	1	70
ν_5	CH stretch	3199	3001	20.8	32.3	0.60			$89S_5$	12	0	88
ν_6	rCH_2 symmetric stretch	3211	3013	4.9	141.5	0.06			$78S_6$, $18S_7$	36	64	0
ν_7	rCH_2 symmetric stretch	3203	3005	12.3	54.0	0.21			$81S_7$, $14S_6$	25	74	1
ν_8	CH_2 antisymmetric stretch	3125	2931	23.4	59.1	0.46			$71S_8$, $28S_9$	6	2	92
ν_9	CH_2 symmetric stretch	3028	2840	78.3	105.2	0.22			$72S_9$, $28S_8$	2	97	1
ν_{10}	NH_2 deformation	1721	1597	33.1	10.7	0.65			$78S_{10}$, $21S_{30}$	67	2	31
ν_{11}	CH_2 deformation	1581	1500	2.6	10.7	0.75			$52S_{11}$, $37S_{12}$	13	14	73
ν_{12}	rCH_2 deformation	1571	1490	0.6	7.1	0.69			$38S_{12}$, $47S_{11}$	77	9	14
ν_{13}	rCH_2 deformation	1528	1450	2.1	8.7	0.75			$99S_{13}$	13	87	0
ν_{14}	CH_2 wag	1493	1409	13.4	4.0	0.53			$34S_{14}$, $17S_{15}$, $15S_{18}$	88	1	11
ν_{15}	CH in-plane bend	1432	1345	9.1	7.7	0.47	1359	1354	$28S_{15}$, $35S_{14}$, $13S_{21}$	99	0	1
ν_{16}	CH_2 twist	1354	1265	4.0	9.9	0.60			$58S_{16}$, $18S_{21}$	96	3	1
ν_{17}	ring breathing	1274	1208	2.6	18.9	0.24			$50S_{17}$, $28S_{14}$	76	12	12
ν_{18}	CC stretch	1290	1197	0.5	4.5	0.69			$11S_{18}$, $18S_{31}$, $16S_{15}$, $15S_{21}$, $10S_{16}$	20	40	40
ν_{19}	rCH_2 twist	1235	1172	0.6	8.2	0.75			$36S_{19}$, $48S_{28}$, $15S_{20}$	4	94	2
ν_{20}	CH out-of-plane bend	1177	1116	2.1	0.6	0.43			$59S_{20}$, $34S_{19}$	0	80	20
ν_{21}	NH_2 twist	1143	1032	9.0	3.3	0.34			$25S_{21}$, $13S_{22}$, $13S_{25}$	3	87	10
ν_{22}	CN stretch	1122	1064	7.3	3.6	0.60	1067	1065	$36S_{22}$, $10S_{30}$	84	13	3
ν_{23}	rCH_2 wag	1106	1050	4.3	0.1	0.75			$73S_{23}$, $19S_{24}$	24	50	26
ν_{24}	rCH_2 wag	1100	1043	11.7	0.8	0.40			$63S_{24}$, $24S_{23}$	76	3	21
ν_{25}	CH_2 rock	1055	980	15.0	7.1	0.26	992		$13S_{25}$, $17S_{22}$	0	82	18
ν_{26}	ring deformation	992	939	9.7	10.4	0.60	931		$38S_{26}$, $15S_{27}$, $12S_{18}$	90	1	9
ν_{27}	ring deformation	953	888	54.2	11.0	0.74			$48S_{27}$, $13S_{30}$	23	74	3
ν_{28}	rCH_2 rock	868	830	2.9	3.3	0.75			$30S_{28}$, $19S_{27}$, $18S_{20}$, $16S_{19}$	5	63	32
ν_{29}	rCH_2 rock	830	805	14.2	2.6	0.45	809		$22S_{29}$, $25S_{26}$, $14S_{18}$, $10S_{25}$	0	81	19
ν_{30}	NH_2 wag	906	771	86.3	7.0	0.55			$32S_{30}$, $23S_{25}$, $13S_{29}$	11	88	1
ν_{31}	rCH_2 twist	799	754	1.4	6.7	0.58			$43S_{31}$, $30S_{29}$, $11S_{26}$	3	44	53
ν_{32}	CCN bend	494	466	7.8	2.5	0.58	471	472	$44S_{32}$, $25S_{35}$	76	2	22
ν_{33}	ring-C in-plane bend	373	352	4.9	1.1	0.26	358	359	$73S_{33}$, $10S_{34}$	47	1	52
ν_{34}	NH_2 torsion	230	207	17.9	0.6	0.75	212	215	$44S_{34}$, $22S_{32}$, $21S_{35}$	24	9	67
ν_{35}	ring-C out-of-plane bend	254	235	32.2	1.4	0.74	235	233[h]	$39S_{35}$, $38S_{34}$, $13S_{32}$	37	1	62
ν_{36}	asymmetric torsion	99	98	4.7	0.2	0.74	103	104	$93S_{36}$	6	37	57

[a] MP2/6-31G(d) predicted values. [b] MP2/6-31G(d) fixed scaled frequencies with factors of 0.88 for CH and NH stretches, 0.70 for CNH bends, 0.75 for amino torsion, 1.0 for asymmetric torsion, and 0.90 for all other modes. [c] Calculated infrared intensities in km/mol from MP2/6-31G(d). [d] Calculated Raman activities in $Å^4$/amu from MP2/6-31G(d). [e] Frequencies from Kr solution at −110 °C. [f] Calculated with MP2/6-31G(d), and contributions of less than 10% are omitted. [g] *A*, *B* and *C* values in the last three columns are percentage infrared band contours. [h] Hydrogen bonding band coincides with this fundamental.

has any symmetry, many of the fundamentals of the other four conformers are expected to give rise to A/B/C hybrid contours. Nevertheless, for each of the conformers, we calculated the expected band contours for each of the fundamentals to aid in the normal mode assignments.

"Group frequencies" for the monosubstituted hydrocarbon ring have been well characterized.[25] They were very valuable for the assignment of the fundamentals of aminomethyl cyclopropane. Also the fundamentals for the $-CH_2NH_2$ group have been confidently assigned[26], providing excellent data for comparisons with those for the substituent on the ring. Therefore, by using all of these data along with the ab initio-predicted infrared and Raman intensities, a reasonably confident vibrational assignment has been provided for the fundamental vibrations for both the Gg-1 and Gt conformers (Tables 1 and 2). Several of the fundamentals for the three less stable conformers have been tentatively identified (Tables 3, 4, and 5).

The most interesting spectral region is below 600 cm^{-1} where the skeletal bending modes are predicted to have significantly different frequencies for gauche and cis conformers for rotation around the C−C bond. For example, the Ct and Cg conformers have a CCN bend in the 520−570 cm^{-1} region, whereas the Gg-1, Gt, and Gg-2 forms have the corresponding vibration predicted at 451, 452, and 466 cm^{-1}, respectively. There are no fundamentals predicted for any of these three forms in the 500−750 cm^{-1} region. Therefore, the weak infrared bands at 529 and 545 cm^{-1} in the rare gas solutions are assigned as the CCN bends for the Ct and Cg conformers, respectively, whereas the 464 and 472 cm^{-1} infrared bands in the rare gas solutions are assigned to the corresponding mode for the gauche (G) forms. The assignments for the 529 and 545 cm^{-1} bands are supported by the relative frequencies from the ab initio predictions as well as from the band contours in the gas phase. The 545 cm^{-1} band has a predicted 49% B-type contour with 19% A-type and 32% C-type contributions. The Q-branches from these two latter contributions simply fill in the minimum in the B-contour. The 529 cm^{-1} band has a predicted 68% A-type character, which gives rise to a strong Q-branch as observed (Figure 4). Similarly, the ring-C in-plane bend is assigned near 360 cm^{-1} for the Gg-1, Gt, and Gg-2 rotamers, whereas the corresponding out-of-plane modes are at 226, 221, and 215 cm^{-1}, respectively. For the Cg and Ct forms, this latter mode is predicted at a significantly higher frequency, whereas the other corresponding fundamental is expected in the 330 cm^{-1} region with extensive mixing of these bends with the NH_2 torsion for these conformers. Because the two cis conformers appear to have a low abundance, the assignment for all three of these latter normal modes is somewhat tentative.

The NH_2 torsion mode is predicted to be at 265 cm^{-1} for the Gg-1 form and observed at 263 cm^{-1} (gas, Figure 4) and 266 cm^{-1} (Kr, Figure 9); this mode is predicted to be 255 cm^{-1} for

TABLE 5: Observed and Calculated Frequencies (cm^{-1}) for *Ct* Aminomethyl Cyclopropane

vib no.	fundamental	ab initio[a]	fix scaled[b]	IR int.[c]	Raman act.[d]	dp ratio	IR gas	IR Kr[e]	PED[f]	*A*[g]	*B*[g]	*C*[g]
ν_1	NH_2 antisymmetric stretch	3634	3409	0.3	33.7	0.75			$100S_1$			100
ν_2	NH_2 symmetric stretch[h]	3527	3308	0.5	63.6	0.07			$100S_2$	69	31	
ν_3	rCH_2 antisymmetric stretch[h]	3300	3096	17.8	28.2	0.56			$99S_3$	59	41	
ν_4	rCH_2 antisymmetric stretch	3289	3085	0.1	69.2	0.75			$99S_4$			100
ν_5	CH stretch[h]	3201	3003	20.1	37.0	0.70			$82S_5$, $18S_6$	0	100	
ν_6	rCH_2 symmetric stretch[h]	3209	3010	1.8	191.3	0.06			$81S_6$, $17S_5$	81	19	
ν_7	rCH_2 symmetric stretch	3204	3005	15.2	19.8	0.75			$100S_7$			100
ν_8	CH_2 antisymmetric stretch	3150	2955	27.6	77.8	0.75			$100S_8$			100
ν_9	CH_2 symmetric stretch[h]	3099	2907	42.0	107.4	0.10			$100S_9$	33	67	
ν_{10}	NH_2 deformation[h]	1724	1599	21.9	5.6	0.74			$77S_{10}$, $22S_{30}$	22	78	
ν_{11}	CH_2 deformation[h]	1554	1474	1.0	12.7	0.73			$98S_{11}$	8	92	
ν_{12}	rCH_2 deformation[h]	1577	1496	2.2	5.2	0.72			$73S_{12}$, $17S_{17}$	20	80	
ν_{13}	rCH_2 deformation	1523	1444	3.8	7.4	0.75			$100S_{13}$			100
ν_{14}	CH_2 wag[h]	1415	1342	17.1	7.1	0.68	1359	1354	$64S_{14}$, $14S_{18}$	100	0	
ν_{15}	CH in-plane bend[h]	1456	1381	3.5	3.6	0.51	1388	1384	$38S_{15}$, $23S_{14}$, $19S_{12}$	57	43	
ν_{16}	CH_2 twist	1430	1314	0.1	9.6	0.75			$54S_{16}$, $37S_{21}$			100
ν_{17}	ring breathing[h]	1279	1213	1.4	18.6	0.23			$48S_{17}$, $28S_{15}$	100	0	
ν_{18}	CC stretch[h]	772	727	12.3	11.7	0.49	715		$35S_{18}$, $34S_{26}$, $15S_{31}$	97	3	
ν_{19}	rCH_2 twist	1235	1172	0.6	8.6	0.75			$34S_{19}$, $44S_{28}$, $20S_{20}$			100
ν_{20}	CH out-of-plane bend	1179	1109	1.3	1.2	0.75	1111		$52S_{20}$, $39S_{19}$			100
ν_{21}	NH_2 twist	1249	1145	1.3	0.8	0.75			$28S_{21}$, $33S_{16}$, $19S_{25}$			100
ν_{22}	CN stretch[h]	1199	1133	5.5	0.6	0.61			$35S_{22}$, $16S_{31}$	28	72	
ν_{23}	rCH_2 wag	1108	1051	1.5	0.1	0.75			$97S_{23}$			100
ν_{24}	rCH_2 wag[h]	1104	1047	8.2	0.6	0.14			$82S_{24}$, $11S_{26}$	0	100	
ν_{25}	CH_2 rock	1003	921	0.4	3.3	0.75			$24S_{25}$, $31S_{27}$, $21S_{21}$			100
ν_{26}	ring deformation[h]	1031	971	58.7	8.9	0.41			$29S_{26}$, $21S_{18}$, $17S_{24}$	94	6	
ν_{27}	ring deformation	897	845	12.0	8.9	0.75			$61S_{27}$, $13S_{25}$			100
ν_{28}	rCH_2 rock	820	769	1.5	1.1	0.75			$32S_{28}$, $28S_{25}$, $16S_{20}$, $15S_{19}$			100
ν_{29}	rCH_2 rock[h]	820	778	1.5	1.5	0.18			$67S_{29}$, $20S_{31}$	95	5	
ν_{30}	NH_2 wag[h]	916	810	219.9	1.5	0.28	810		$52S_{30}$, $17S_{10}$, $15S_{26}$, $14S_{22}$	81	19	
ν_{31}	rCH_2 twist[h]	1081	1024	2.1	7.6	0.74			$24S_{31}$, $35S_{22}$, $17S_{29}$, $12S_{15}$	98	2	
ν_{32}	CCN bend[h]	550	520	16.0	3.0	0.75	531	529	$46S_{32}$, $28S_{33}$, $10S_{31}$	68	32	
ν_{33}	ring-C in-plane bend[h]	274	260	1.4	0.5	0.16			$60S_{33}$, $37S_{32}$	3	97	
ν_{34}	NH_2 torsion	368	337	33.1	2.5	0.75	332	331	$59S_{34}$, $33S_{35}$			100
ν_{35}	ring-C out-of-plane bend	333	301	24.6	0.7	0.75	307	303	$56S_{35}$, $36S_{34}$			100
ν_{36}	asymmetric torsion	118	118	2.7	0.2	0.75	125	125	$97S_{36}$			100

[a] MP2/6-31G(d) predicted values. [b] MP2/6-31G(d) fixed scaled frequencies with factors of 0.88 for CH and NH stretches, 0.70 for CNH bends, 0.75 for amino torsion, 1.0 for asymmetric torsion, and 0.90 for all other modes. [c] Calculated infrared intensities in km/mol from MP2/6-31G(d). [d] Calculated Raman activities in $Å^4$/amu from MP2/6-31G(d). [e] Frequencies from Kr solution at −110 °C. [f] Calculated with MP2/6-31G(d), and contributions of less than 10% are omitted. [g] *A*, *B*, and *C* values in the last three columns are percentage infrared band contours. [h] Indicates a mode in the A′ symmetry block.

the Gt form and observed at 247 cm^{-1} (gas, Figure 4) and 251 cm^{-1} (Kr, Figure 9), the 10 (predicted), 15 (Kr) and 16 (gas) cm^{-1} differences is far beyond the average 1% error expected. Thus, we believe our assignment of the conformer pairs is justified. The predicted frequencies for the asymmetric torsions range from a high value of 139 cm^{-1} (Cg) to a low value of 98 cm^{-1} (Gg-2) with values of 127, 122, and 118 cm^{-1} for the other conformers. There is a broad infrared band in the krypton solution at about 130 cm^{-1}, which is undoubtedly due to this mode. As the temperature is lowered, the intensity grows at about 135 cm^{-1}, whereas at the warmer temperature of −85 °C the maximum is evident at 132 cm^{-1}. These maxima have been assigned to the asymmetric torsions for the Gg-1 and Gt conformers, respectively, whereas a questionable shoulder at 145 cm^{-1} is assigned to this mode for the Cg form.

In the "fingerprint" region, particularly for the spectra between 900 and 1200 cm^{-1}, many of the assignments were strongly influenced by the ab initio predicted frequencies. Also, it should be noted that the descriptions provided in many cases are more for bookkeeping than for giving the major atomic motions involved. Many of these vibrations have three or four significant symmetry coordinate contributions and their relative order differs among the five conformers. Therefore, further discussion of these assignments is not warranted.

For some of the conformers, there is extensive mixing as might be expected for a molecule without any symmetry. For

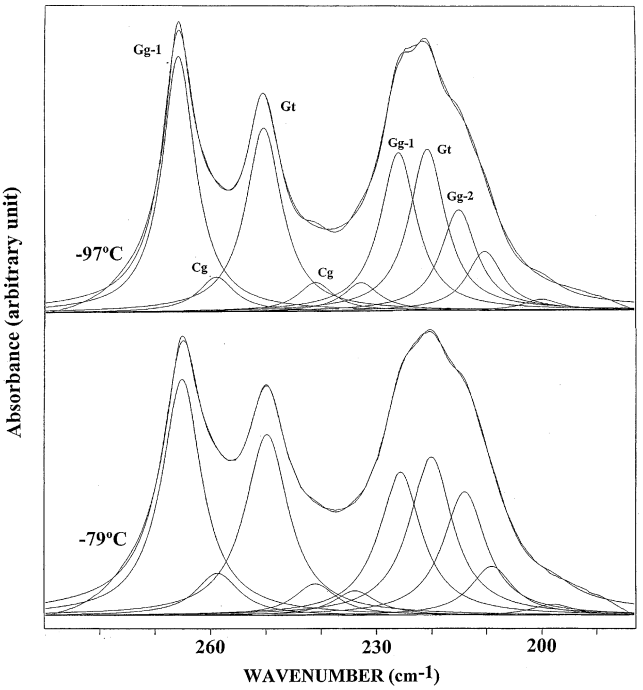

Figure 9. Resolution of bands and their temperature dependence (at −79 and −97°C) in the far-infrared spectra of aminomethyl cyclopropane dissolved in liquid krypton in the range 290−183 cm^{-1}.

TABLE 6: Calculated Energies (Hartree) and Energy Difference (cm^{-1}) for the Five Conformers of Aminomethyl Cyclopropane

method/basis set	cis-trans	cis-gauche	gauche-trans	gauche-gauche−1	gauche-gauche−2
RHF/6-31G(d)	−211.113127	−211.113702	−211.115456	−211.115530	−211.113665
	527	**401**	**16**	**0**	**409**
MP2/6-31G(d)	−211.820671	−211.820969	−211.822197	−211.821758	−211.819771
	239	**173**	**−96**	**0**	**436**
MP2/6-31+G(d)	−211.835636	−211.836488	−211.837856	−211.838136	−211.836236
	549	**362**	**61**	**0**	**417**
MP2/6-311G(d,p)	−212.044555	−212.045106	−212.046126	−212.045510	−212.043852
	210	**89**	**−135**	**0**	**364**
MP2/6-311+G(d,p)	−212.051800	−212.052413	−212.053779	−212.053941	−212.052298
	470	**335**	**36**	**0**	**361**
MP2/6-311G(2d,2p)	−212.105284	−212.105889	−212.106626	−212.106294	−212.104520
	222	**89**	**−73**	**0**	**389**
MP2/6-311+G(2d,2p)	−212.110886	−212.111491	−212.112906	−212.113041	−212.111375
	473	**340**	**30**	**0**	**336**
MP2/6-311G(2df,2pd)	−212.191986	−212.192475	−212.193216	−212.192892	−212.191119
	199	**92**	**−71**	**0**	**389**
MP2/6-311+G(2df,2pd)	−212.196896	−212.197399	−212.198859	−212.198968	−212.197310
	455	**344**	**24**	**0**	**364**
B3LYP/6-31G(d)	−212.551459	−212.550913	−212.553080	−212.552324	−212.550374
	190	**476**	**−166**	**0**	**428**
B3LYP/6-31+G(d)	−212.561990	−212.562098	−212.564328	−212.564192	−212.562408
	483	**460**	**−30**	**0**	**392**
B3LYP/6-311G(d,p)	−212.616682	−212.616558	−212.618257	−212.617593	−212.615784
	200	**227**	**−146**	**0**	**397**
B3LYP/6-311+G(d,p)	−212.621115	−212.621217	−212.623262	−212.623166	−212.621548
	450	**428**	**−21**	**0**	**355**
B3LYP/6-311G(2d,2p)	−212.625826	−212.625775	−212.627308	−212.626748	−212.625087
	203	**214**	**−123**	**0**	**365**
B3LYP/6-311+G(2d,2p)	−212.629827	−212.629916	−212.632038	−212.631926	−212.630443
	461	**441**	**−25**	**0**	**325**
B3LYP/6-311G(2df,2pd)	−212.632096	−212.632096	−212.633566	−212.633052	−212.631416
	210	**210**	**−113**	**0**	**359**
B3LYP/6-311+G(2df,2pd)	−212.635923	−212.636011	−212.638147	−212.638047	−212.636579
	466	**447**	**−22**	**0**	**322**

example, the Gt conformer has four fundamentals that have contributions from five different symmetry coordinates with the maximum contribution from any one of them in the mid-thirty percent range (Table 2). For the Gg-1 conformer, there are six bands which have contributions from four symmetry coordinates where three of them have maximum contribution from any one symmetry coordinate of 23% or less (Table 1). For the other three conformers, the mixing is not as extensive. We have kept the numbering for each normal mode for all five conformers the same, but the frequency may be significantly different because the mixing varies depending on the conformer.

The assignments for the carbon−hydrogen and nitrogen−hydrogen stretches is rather straightforward. The C−H modes of the ring are significantly separated from those for the $-CH_2N$ group with little separation between the two ring CH_2 antisymmetric stretches or the two corresponding symmetric modes. The NH_2 stretches are very weak in the infrared spectra and only those for the Gg-1 and Gt conformers were observed.

Conformational Stability. To determine the conformational stabilities for five possible conformers of aminomethyl cyclopropane, it is necessary to identify vibrational bands due to the three less stable forms where such identifications are hampered in the krypton solution by hydrogen bonding. Therefore, bands due to the most abundant two conformers were initially identified. Many overtone and combination bands are possible because of the large number of conformers present. Therefore, the lowest frequency modes with the fewest possible interfering bands were chosen for the ΔH determinations. Also, intense bands need to be used so the krypton solution can be as dilute as possible to minimize the hydrogen bonding. With these criteria, the most logical bands are the two strong bands at 266 and 251 cm^{-1}, which are assigned as ν_{34} for the Gg-1 and Gt conformers, respectively, with predicted frequencies of 265 and 255 cm^{-1} and intensities of 48.8 and 44.6 km/mol, respectively. Spectral deconvolution of part of the far-infrared spectrum of the krypton solution recorded at −79 °C and −97 °C is shown in Figure 9. The standard curve fit software (OPUS/IR program version 2.2, which uses the Levenberg-Marquadt algorithm) of the Bruker FT-IR instrument was used to separate the conformer bands. There is obviously a weak band on the low frequency shoulder of the 265 cm^{-1} band at 258 cm^{-1} that is assigned as this same fundamental for the Cg form with a predicted frequency of 262 cm^{-1} and intensity of 21.2 km/mol. There is also a weak shoulder on the 251 cm^{-1} band at 241 cm^{-1} that is assigned as ν_{33} of the Cg conformer.

The other strong band in this spectral region is the ring-C bend that is centered at about 222 cm^{-1} and made up of three relative pronounced bands (Figure 9) at 226, 221, and 215 cm^{-1} and a weaker band at 209 cm^{-1}. The higher frequency band at 226 cm^{-1} is assigned to the most stable conformer based on the fact that it becomes more intense as the temperature is lowered, whereas the 221 cm^{-1} band has decreasing intensity. The 215 cm^{-1} band is assigned to the Gg-2 conformer. With these assignments, the enthalpy differences were determined for four conformer pairs to evaluate the relative stabilities of the Gg-1, Gt, and Cg conformers (Table 7). For the Gt conformer, when the intensity of its two bands are compared to the intensity of the 266 cm^{-1} band of the Gg-1 form, the ΔH values are relatively low compared to the values obtained with the band of Gg-1 at 226 cm^{-1}. However, by combining the data from all four intensity ratios an average value of 109 ± 7 cm^{-1} was obtained with the Gg-1 conformer as the more stable form. For the Cg conformer, the average value for the four determinations is 267 ± 28 cm^{-1}.

TABLE 7: Temperature and Intensity Ratios from the Study of the Five Conformers of Aminomethyl Cyclopropane Dissolved in Liquid Krypton

		Gg-1/Gt				Gg-1/Cg				Gg-1/Gg-2		Gg-1/Ct			
T (°C)	1000/T (K^{-1})	I_{266}/I_{251}	I_{266}/I_{221}	I_{226}/I_{251}	I_{226}/I_{221}	I_{266}/I_{241}	I_{266}/I_{258}	I_{226}/I_{241}	I_{226}/I_{258}	I_{266}/I_{215}	I_{226}/I_{215}	I_{266}/I_{303}	I_{226}/I_{303}	I_{266}/I_{529}	I_{226}/I_{529}
−79.0	5.1507	1.3007	1.4812	0.7786	0.8866	7.4026	5.5893	4.4311	3.3457	1.9008	1.1378	3.3742	2.0197		
−82.0	5.2315	1.3342	1.4858	0.7914	0.8813	8.1363	6.5258	4.8264	3.8710	1.9870	1.1787	3.8452	2.2809	18.7329	31.5797
−85.0	5.3149	1.3375	1.4976	0.8062	0.9027	8.4087	6.8312	5.0685	4.1176	2.1331	1.2858	3.8352	2.3117	19.1035	31.6933
−88.0	5.4010	1.3392	1.5051	0.8093	0.9095	8.4398	6.6732	5.1000	4.0325	2.1655	1.3086	4.1767	2.5239	19.6934	32.5899
−91.0	5.4900	1.3490	1.5147	0.8325	0.9348	8.6011	6.9136	5.3081	4.2667	2.2379	1.3811	4.4008	2.7159	21.1549	34.2786
−94.0	5.5819	1.3576	1.5233	0.8436	0.9466	8.5061	6.7530	5.2859	4.1965	2.3657	1.4701	4.4738	2.7801	21.8363	35.1389
−97.0	5.6770	1.3838		0.8633	0.9789	8.6245	7.2344	5.3806	4.5133	2.5077	1.5645	4.9310	3.0763	24.5780	39.3959
−100.0	5.7753			0.8730		10.3681		6.0424		2.8685	1.6717	5.1801	3.0189	26.0463	44.6926
−103.0	5.8772			0.8894		10.1586				3.0040	1.7013			27.9799	49.4044
−106.0	5.9827			0.9049						3.0892	1.7353			29.0212	51.6628
−109.0	6.0920													31.8143	55.8369
−112.0	6.2054													34.2228	63.0513
ΔH(cm^{-1})		65 ± 11	47 ± 2	127 ± 3	135 ± 15	263 ± 49	239 ± 81	267 ± 41	307 ± 74	423 ± 24	376 ± 20	441 ± 34	456 ± 43	452 ± 15	528 ± 31
ΔH(cm^{-1}) average		**109 ± 7**				**267 ± 28**				**400 ± 16**		**480 ± 15**			

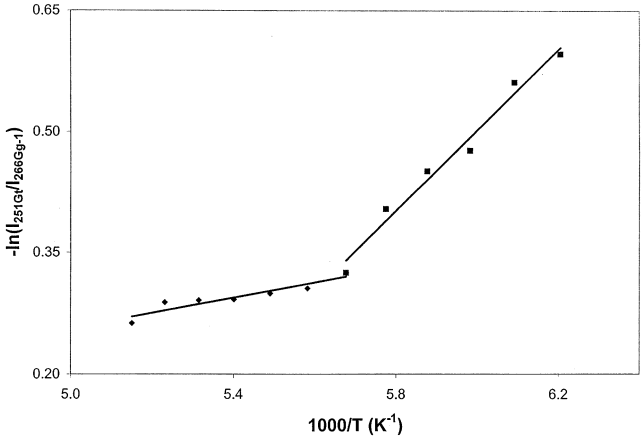

Figure 10. Dimerization/hydrogen bonding from the van't Hoff plot of intensity ratios of amino torsion (266 cm^{-1} Gg-1 band and 251 cm^{-1} Gt band) of aminomethyl cyclopropane. ◆, monomer; ■, dimer.

The 215 cm^{-1} band of the Gg-2 conformer was then used with the 266 and 226 cm^{-1} bands of the Gg-1 conformer to obtain the enthalpy difference for the Gg-2 conformer. The results were 423 ± 24 and 376 ± 20 cm^{-1} with an average of 400 ± 16 cm^{-1}. For the Ct conformer, the weak band at 303 cm^{-1}, which is undoubtedly the ring-C bend for this form, has been used for the enthalpy determination along with the band at 529 cm^{-1}. The four determined values result in an average value of 480 ± 15 cm^{-1}. Assuming a 10 % uncertainty rather than the statistical uncertainties for these determinations gives values of 109 ± 11, 400 ± 40, and 480 ± 48 cm^{-1} for the Gt, Gg-2, and Ct conformers, respectively, relative to the most stable Gg-1 form.

From the variable temperature study of the NH_2 torsion, it is clear that the slope of the relative intensity of the 261 cm^{-1} band changes dramatically at about −115 °C (Figure 10). This change cannot be the result of the sample freezing, because low frequency lattice modes were not observed, and additionally, there was no increase in the amino torsion frequency of ∼200 cm^{-1} as expected for the solid phase. We believe this change in ΔH is mainly the result of the hydrogen-bonding related dimerization. Thus, the major change in the slope beginning at about −115 °C can be attributed to the difference in the enthalpy of hydrogen-bonding-related dimerization for different conformers, and we obtained this difference as the temperature was lowered to −150 °C. From the van't Hoff equation, the ΔH value for the dimerization is 348 ± 26 cm^{-1}, which is probably strongly correlated to the energy of hydrogen bonding. This value is consistent with the value of 530 ± 29 cm^{-1} for hydrogen bonding in methylamine, which was obtained from variable temperature infrared spectra of krypton solutions.[26]

Structural Parameters. We have found that we can obtain good structural parameters by adjusting the structural parameters obtained from the ab initio calculations to fit the rotational constants obtained from the microwave experimental data (computer program A&M, Ab initio and Microwave,[27] developed in our laboratory). To reduce the number of independent variables, the structural parameters are separated into sets according to their types. Bond lengths in the same set keep their relative ratio, and bond angles and torsional angles in the same set keep their differences in degrees. This assumption is based on the fact that the errors from ab initio calculations are systematic.

Unfortunately, the microwave spectra of only two conformers, Gg-1 and Gt, have been reported[18], and only for the normal species. Therefore, there are only six rotational constants available, so only six structural parameters can be determined. However, we have found that the MP2/6-311+G(d,p) ab initio calculations predict the C−H distances within 0.002 Å of the r_0 values determined from the isolated C−H stretching frequencies[28] for a significant number of monosubstituted hydrocarbons.[29] Therefore, these parameters can be fixed to the ab initio-predicted values. Because the heavy atom distances and angles have a more pronounced effect on the rotational constants than the hydrogen atoms parameters, five such parameters (carbon−carbon and carbon−nitrogen distances and the three skeletal angles ∠CCC, ∠CCN, and τNCCC (dihedral)) were selected for the adjustment. The N−H distances were fixed at the ab initio MP2/6-311+G(d,p) values, which are probably too long by 0.005 Å. Nevertheless, reducing them by this amount does not significantly affect the heavy atom parameters.

The parameters obtained by this method are listed in Table 8. It is estimated that these heavy atom distances should be accurate to ±0.005Å and the carbon−hydrogen distances to ±0.003Å. The angles are expected to be within ±0.5°, with the possible exception of the dihedral angles for which the ab initio calculations are the least sensitive. The N−C distances have values similar to those reported for this parameter (1.462 ± 0.005Å) for dimethylamine.[30] The fit of the six rotational constants is given in Table 8 and the agreement with the experimental rotational A constants is within 4 and 5 MHz for the Gg-1 and Gt conformers, respectively, with about one-half these differences for the B and C rotational constants, which have values about one-fourth those of the A constants.

There are some significant differences between these adjusted r_0 parameters and those estimated previously by transferring structural parameters from related compounds with adjustments

TABLE 8: Structural Parameters (Å and Degree), Rotational Constants (MHz) and Dipole Moments (Debye) for *Gg-1* and *Gt* Rotamers of Aminomethyl Cyclopropane

	MP2/6-311+G(d,p)		Microwave[a]		adjusted r_0	
	Gg-1	Gt	Gg-1	Gt	Gg-1	Gt
$r(C_1C_2)$	1.5056	1.5068	1.512[b]	1.512[b]	1.5078	1.5091
$r(C_1C_3)$	1.5100	1.5085	1.512[b]	1.512[b]	1.5144	1.5129
$r(C_2C_3)$	1.5118	1.5120	1.512[b]	1.512[b]	1.5141	1.5143
$r(C_1C_4)$	1.5041	1.5113	1.520[b]	1.520[b]	1.5065	1.5137
$r(C_4N_5)$	1.4650	1.4636	1.472[b]	1.472[b]	1.4626	1.4612
$r(C_2H_6)$	1.0845	1.0847	1.083[b]	1.083[b]	1.0845	1.0847
$r(C_2H_7)$	1.0832	1.0834	1.083[b]	1.083[b]	1.0832	1.0834
$r(C_3H_8)$	1.0854	1.0855	1.083[b]	1.083[b]	1.0854	1.0855
$r(C_3H_9)$	1.0834	1.0835	1.083[b]	1.083[b]	1.0834	1.0835
$r(C_1H_{10})$	1.0858	1.0877	1.083[b]	1.083[b]	1.0858	1.0877
$r(C_4H_{11})$	1.1026	1.0965	1.093[b]	1.093[b]	1.1026	1.0965
$r(C_4H_{12})$	1.0954	1.0954	1.093[b]	1.093[b]	1.0954	1.0954
$r(N_5H_{13})$	1.0151	1.0157	1.017[b]	1.017[b]	1.0151	1.0157
$r(N_5H_{14})$	1.0154	1.0152	1.017[b]	1.017[b]	1.0154	1.0152
$\angle C_1C_2C_3$	60.06	59.96	60.0[b]	60.0[b]	60.15	60.05
$\angle C_1C_3C_2$	59.77	59.85	60.0[b]	60.0[b]	59.72	59.80
$\angle C_2C_1C_3$	60.18	60.19	60.0[b]	60.0[b]	60.13	60.14
$\angle C_2C_1C_4$	119.63	119.66			118.47	118.51
$\angle C_3C_1C_4$	118.75	118.83			119.50	119.58
$\angle C_1C_4N_5$	109.84	115.61	110.0(15)	116.0(15)	109.99	115.75
$\angle H_6C_2H_7$	115.04	115.02	116.0[b]	116.0[b]	115.04	115.02
$\angle H_8C_3H_9$	115.11	115.04	116.0[b]	116.0[b]	115.11	115.04
$\angle C_4C_1H_{10}$	114.69	115.16	116.0[b]	116.0[b]	114.94	115.41
$\angle C_1C_4H_{11}$	108.07	108.44	109.47[b]	109.47[b]	108.07	108.44
$\angle C_1C_4H_{12}$	109.81	109.91	109.47[b]	109.47[b]	109.81	109.91
$\angle C_4N_5H_{13}$	110.69	109.49	109.47[b]	109.47[b]	110.69	109.49
$\angle C_4N_5H_{14}$	109.46	109.92	109.47[b]	109.47[b]	109.46	109.92
$\angle H_{13}N_5H_{14}$	107.22	106.52	109.47[b]	109.47[b]	107.22	106.62
$\tau N_5C_4C_1C_2$	−154.98	−151.51	−151(3)	−149(3)	−155.63	−152.17
$\tau H_{13}N_5C_4C_1$	179.60	54.09	180.0[b]	60.0[b]	179.60	54.09
$\tau H_{14}N_5C_4C_1$	61.63	−62.59	60.0[b]	−60.0[b]	61.63	−62.59
A	12319.2	12209.3	12292.3316(51)	12173.1806(50)	12287.7	12178.4
B	3217.1	3169.7	3202.9457(14)	3162.6582(13)	3206.5	3159.2
C	2877.5	2854.2	2865.8045(12)	2846.8065(12)	2867.7	2845.0
$\lvert\mu_a\rvert$	0.175	1.213	0.144(2)	1.018(26)	0.174	1.202
$\lvert\mu_b\rvert$	0.044	0.438	0.000[b]	0.39(16)	0.060	0.457
$\lvert\mu_c\rvert$	1.291	0.938	1.068(16)	0.833(55)	1.293	0.932
$\lvert\mu_t\rvert$	1.304	1.594	1.077(16)	1.372(60)	1.306	1.588

[a] Ref 17. [b] Assumed parameters.

of the ∠CCN angles and the dihedral $\tau N_5C_4C_1C_2$ angles to fit the six microwave rotational constants.[18] There is a clear indication that the two carbon−hydrogen distances of the methylene group differ by 0.007 Å for the Gg-1 conformer, whereas they were previously assumed to be equal. Also, the C_1-C_4 distance for the Gg-1 form is 0.007 Å shorter than the corresponding distance in the Gt conformer, whereas they were previously assumed to be the same. Most of the remaining parameters estimated earlier[18] from the microwave data are in reasonable agreement with the adjusted r_0 parameters. Also, there is excellent agreement of the two previously determined parameters for the two conformers, although their estimated uncertainties were rather large. For the $\angle C_1C_4N$ angle, values of 110.0 ± 1.5° and 116.0 ± 1.5° for the Gg-1 and Gt conformers, respectively, were reported, whereas the values currently obtained are 110.0 ± 0.5° and 115.8 ± 0.5°, respectively. Similarly, the reported dihedral angles had values of −151 ± 3° and −149 ± 3°, whereas the r_0 adjusted values are −155.6 ± 0.5° and −152.2 ± 0.5°, respectively, for the Gg-1 and Gt forms.

By utilizing the adjusted r_0 parameters from the Gg-1 and Gt conformers with the predicted differences between those from the MP2/6-311+G(d,p) ab initio calculations for the Gg-2, Ct, and Cg forms (Table S2), it should be possible to estimate the values of the A, B, and C rotational constants accurately for the three less stable conformers. With these better estimates, it should be possible to assign the microwave lines for the three less stable conformers, particularly if one uses FT-microwave equipment. Such studies would be useful to obtain even more accurate structural parameters for the heavy atoms of aminomethyl cyclopropane with the availability of an additional nine rotational constants.

The major predicted structural difference among the conformers is for the C_1-C_4 bond distance, which ranges from a low value of 1.505 Å for the Gg-2 conformer to a high value of 1.522 Å for the Ct conformer, which is a very large difference for conformers. For the two most stable conformers, the bond length difference is only 0.007 Å with the more stable Gg-1 conformer having the shorter bond of 1.507 Å. The variation in the C_4-N distance is only 0.005 Å for four of the five conformers, with the Ct conformer having the very short 1.458 Å distance (Table S2). With the exception of these indicated distances, most of the other distances have very small predicted variations with exception of the C_4-H distances for two of the conformers. However, there are some very large predicted variations of the angles among the conformers in addition to the dihedral angles. The $\angle ringC_1C_4$ angle exhibits the most significant differences between the heavy atom gauche and cis conformations, this angle is predicted to be 124.3°, 124.4°, and 124.3° respectively, for the Gg-1, Gt, and Gg-2 forms; and

significantly larger values of 126.6° and 127.8° for the Cg and Ct forms, respectively. Also to be noted is the $\angle C_1C_4N_5$ angles, which differ significantly between the amino trans and gauche conformations, this angle is predicted to be 109.8°, 110.6°, and 111.7°, respectively, for the Gg-1, Gg-2, and Cg forms; and significantly larger values of 115.6° and 117.7° for the Gt and Ct forms, respectively.

Discussion

There is little question that the Gg-1 and Gt conformers are the two most stable forms of aminomethyl cyclopropane, and the variable temperature study indicates that the Gg-1 form is the more stable rotamer of this pair. This result is in agreement with the proposed stability from the microwave study.[18] It agrees with the prediction from the MP2 calculations only when diffuse functions are used with all four basis sets, i.e., 6-31+G(d), 6-311+G(d,p), 6-311+G(2d,2p), 6-311+G(2df,2pd). When diffuse functions are not used, the Gt conformer is predicted to be more stable by a low value of 71 cm^{-1}, with the largest basis set to a high value of 135 cm^{-1} with the 6-311G(d,p) basis set. Thus, the diffuse function favors the gauche conformer of the NH_2 group by at least 100 cm^{-1}, with the Gg-1 form estimated to be about 30 cm^{-1} lower in energy than the Gt form. However, density functional theory calculations performed predict the Gt conformer to be the more stable form by about 20 cm^{-1} with diffuse functions and 120 cm^{-1} without them (Table 6). The Cg form is predicted to be the third most stable form with the energy difference from the MP2 calculation with the diffuse functions in agreement with the experimentally determined enthalpy difference.

It is interesting that by using diffuse functions for predicting the conformational stability of ethylamine,[14] the gauche conformer is predicted to be more stable, whereas, experimentally, the trans rotamer is the more stable conformer. However, for aminomethyl cyclopropane, it appears that diffuse functions must be used to predict the correct conformational stability. Higher level calculations for both of these molecules would be very useful to determine if one could give some criteria when diffuse functions should be used for correctly predicting the conformational stability of organoamines.

Taking into account the double degeneracy of all the forms except the Ct conformer, it is estimated that the relative abundances for each conformer at ambient temperature are 49% Gg-1, 29% Gt, 13% Cg, 7% Gg-2, and 2% Ct. These percentages seem to be consistent with the relative infrared band intensities for the various identified conformer bands when the predicted ab initio intensities are taken into consideration. Because the Gg-2 and Ct conformers have such low abundance, only a limited number of their fundamentals could be identified, and it was mainly the low-frequency ones which could be assigned with confidence.

In the microwave investigation[18] of aminomethyl cyclopropane, two excited states of the Gg-1 conformer were assigned, and from their relative intensities the frequencies for the vibrational modes from which these excited states arose were obtained as 159 ± 20 and 259 ± 30 cm^{-1}. The lower frequency was assigned to the C−C torsional mode and the higher frequency to the CCN bending mode. This assignment was based on the A − C difference of rotational constants upon excitation, which is expected to be relatively small for the NH_2 torsional mode. The observed frequencies for these two modes are 129 and 222 cm^{-1}, respectively, for the Gg-1 conformer, which indicates that the reported microwave uncertainties were too conservative, because the actual differences are 30 and 37 cm^{-1} from the observed values.

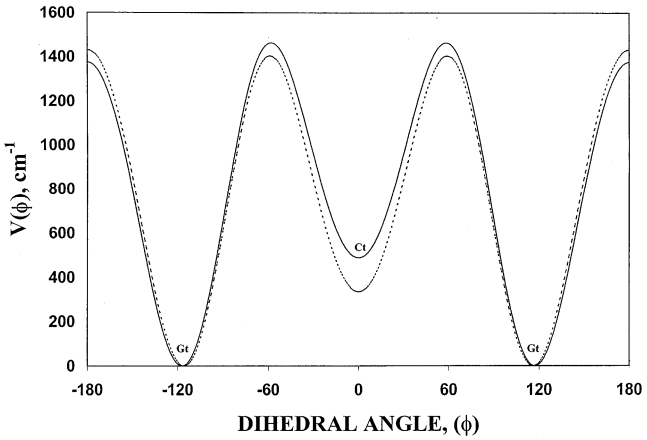

Figure 11. Calculated potential functions (solid curve, from MP2(full)/6-31+G(d);, and dotted curve, from MP2(full)/6-31G(d)) governing asymmetric torsion in aminomethyl cyclopropane (with amino trans orientation). Dihedral angle 0° defined for the Ct conformer.

For the Gt conformer, similar excited states were observed, and from their relative intensities, the predicted frequencies for the corresponding modes were 148 ± 20 and 229 ± 30 cm^{-1}. The observed frequencies are 125 and 218 cm^{-1}. The lower frequency band differs by 23 cm^{-1}, whereas the higher frequency band differs by only 11 cm^{-1}. Although these differences are much smaller, the lower frequency band is still outside the estimated value from the microwave study. Nevertheless, the vibrational assignments for these four bands from the microwave study were correct, but the data clearly show the difficulty in obtaining intensity measurements from microwave spectra.

For a significant number of molecules, we have found that the ab initio predictions with the 6-31G(d) basis set at the MP2 level provide potential functions that have barriers to conformer interconversions that agree well with those obtained from the experimental data of the torsional frequencies for the two different conformers (gauche and cis/trans forms) along with the ΔH value and the gauche dihedral angle. In most cases, the differences between the experimental and predicted barriers are smaller than 200 cm^{-1}. Therefore, we have predicted the barriers between the Gt and Ct conformers (Figure 11) with ab initio calculations. The predicted potential function from MP2/6-31+G(d) basis set is nearly 3-fold, with an energy difference between the conformers of 487 cm^{-1} with a gauche to gauche barrier of 1375 cm^{-1} and a gauche to cis barrier of 1463 cm^{-1}. We also carried out a similar calculation without diffuse functions utilizing the 6-31G(d) basis set, this resulted in a conformation difference of 334 cm^{-1}, a gauche to gauche barrier of 1431 cm^{-1} and a gauche to cis barrier of 1403 cm^{-1} (Figure 11). There is no significant difference in the potential functions governing the conformational interchange from Gt to Ct between these two ab initio predicted values. Thus, it is expected that the predicted potential function should be very similar to the actual potential for conformational interchange. This torsional potential can be represented as a Fourier cosine series in the internal angle (ϕ): $V(\phi) = \sum_{i=1}^{5} (V_i/2)(1 - \cos i\phi)$, the first five terms of the series were used to approximate this potential function and the corresponding coefficients V_1 through V_5 were determined (Table 9).

We have also predicted the potential function governing the conformational interchange of the NH_2 group by predicting the energies of Gt, Gg-1, and Gg-2 conformers as well as three amino torsional transition maxima. Again ab initio MP2/6-31G(d) and MP2/6-31+G(d) calculations with full electron correlation were carried out. The resulting potential function

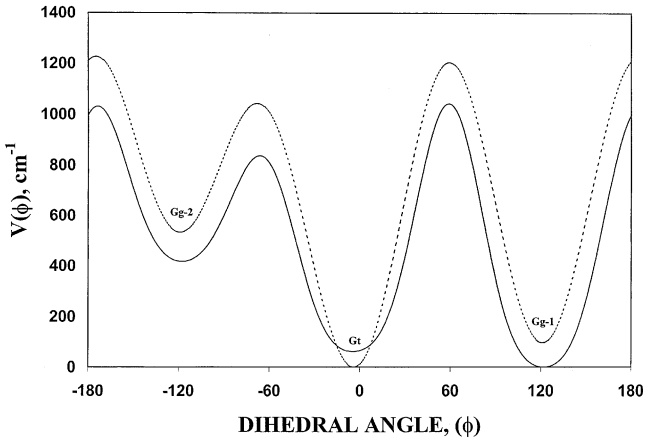

Figure 12. Calculated potential functions (solid curve, from MP2(full)/6-31+G(d), and dotted curve, from MP2(full)/6-31G(d)) governing amino torsion in aminomethyl cyclopropane (with asymmetric torsion gauche orientation). Dihedral angle near 0° defined for the Gt conformer.

TABLE 9: Potential Barriers (cm^{-1}) and Fourier Coefficients (cm^{-1}) Associated with the Asymmetric Torsion of Aminomethyl Cyclopropane Determined from Predicted from ab Initio Energies

coefficients	MP2(Full)/6-31+G(d)	MP2(Full)/6-31G(d)
V_1	−286	−92
V_2	−273	−266
V_3	1264	1289
V_4	11	34
V_5	−91	−102
potential barriers		
Gt → Gt	1375	1431
Gt → Ct	1463	1403
Ct → Gt	976	1068

TABLE 10: Potential Barriers (cm^{-1}) and Fourier Coefficients (cm^{-1}) Associated with the Amino Torsion of Aminomethyl Cyclopropane Determined from Predicted ab Initio Energies

coefficients	MP2(Full)/6-31+G(d)	MP2(Full)/6-31G(d)
V_1	157	267
V_2	67	135
V_3	788	926
V_4	−19	−3
V_5	−13	5
V_6	−122	−2
V_1'	−178	−143
V_2'	370	361
V_3'	1	44
V_4'	−4	−4
V_5'	−71	−5
potential barriers		
Gg-1 → Gt	1042	1108
Gg-1 → Gg-2	1032	1131
Gt → Gg-1	981	1204
Gt → Gg-2	776	1043
Gg-2 → Gg-1	615	695
Gg-2 → Gt	420	511

(Figure 12) is asymmetric, because rotation of amino group with heavy atom gauche orientation yields two distinct amino gauche forms. With utilization of a Fourier series consisting of the first six cosine and five sine functions in the form: $V = 1/2 [\sum_{k=1}^{6} V_k(1 - \cos k\phi) + \sum_{k=1}^{5} (V'_k \sin k\phi)]$, the corresponding potential coefficients were obtained for the two basis sets with and without diffuse functions (Table 10). The inclusion of diffuse functions predicted the Gg-1 form more stable than the Gt form, which agrees with the experimental result, whereas the exclusion of diffuse functions lead to an erroneous order of predicted conformational stability. Aside from this effect, the two predicted potential functions are very similar. The predicted barriers to internal rotation are listed in Table 10.

Because there are only a few of the structural parameters that have significantly different values among the five conformers, there are only a limited number of the force constants with differences greater than 5%. For the stretching force constants, these are the C_1-C_4, C_4-H_{11}, and N_5-H_{14} bonds. For the C_1-C_4 bond, the two conformers that have the NH_2 group trans have values of 5.5% (Gt) and 7.1% (Ct) smaller than the value of this force constant for the Gg-1 form (Table S3). For the C_4-H_{11} force constant, it is larger by 6.6% (Gt), 7.2% (Ct) and 6.9% (Gg-2) compared to the corresponding one for Gg-1. For the N_5-H_{14} bond, the value for this force constant is smaller by 5.4% (Ct), 5.8% (Cg), 6.7% (Gt), and 6.9% (Gg-2) than the value of 6.626 mdyn/Å for this force constant for the Gg-1 conformer (Table S3). For the bending force constants, those for the $C_2C_1C_4$ and $C_1C_4N_5$ angles for the Cg form are 23.7 and 25.9% larger, respectively, and for the Ct rotamer, 17.3 and 26.3% larger, respectively, than the corresponding constant for the Gg-1 conformer. Smaller differences for $\angle C_3C_1C_4$ of 6.2 and 9.9% and $\angle C_4C_1H_{10}$ of 10.9% and 9.6% for the Cg and Ct conformers, respectively, compared to those for the Gg-1 rotamer were obtained. For most of the other force constants, the values vary by less than 1% among the five conformers. For this reason, most of the fundamental vibrations have very similar values for the five forms, which made it difficult to identify a significant number of conformer bands for each form.

The predicted frequencies from the ab initio MP2/6-31G(d) calculations agree to better than 1% for the bands that could be clearly identified for each conformer with only four scaling factors. For the hydrocarbon portion of most molecules, only two scaling factors are needed to predict the normal vibrations of this moiety and multiple scaling factors are not necessary to obtain predicted wavenumbers to better than 1%. However, for organoamines, two additional force constants are needed for the CNH bend and the amino torsion.

A comparison of the determined conformational stabilities between aminomethyl cyclopropane $c-C_3H_5CH_2NH_2$ and allylamine[31] $CH_2{=}CHCH_2NH_2$ molecules is interesting because both molecules exhibit the same five conformations resulting from rotation around the C−C and C−N bonds. From recent variable temperature studies of the infrared spectra of rare gas solutions, we[31] found that the Ct form is the most stable conformation for allylamine, Gt, Gg-1, and Cg forms are determined to be the second, third, and fourth most stable conformation, with enthalpy differences of 92 ± 8 cm^{-1}, 122 ± 12 cm^{-1}, and 173 ± 12 cm^{-1} compared to the Ct form, respectively. No spectroscopic evidence was obtained for the Gg-2 form, which is predicted by most of the ab initio calculations to be less stable by more than 600 cm^{-1} than the Ct form. The difference in the stability ordering clearly arises from the different electronic properties of the cyclopropyl and ethynyl moieties and the consequent different interactions with the rest of the molecules.

Marstokk and Møllendal,[18] in their microwave investigation of aminomethyl cyclopropane, proposed the repulsion between the pseudo-π electrons of the three-membered ring and the lone electron pair on the nitrogen atom be the major factor leading to the lower stability of the Gg-2 and Cg forms, while intramolecular hydrogen-bonding between the pseudo-π electrons of the three-membered ring and the hydrogen atoms from the amino group leads to the higher stability of Gg-1 and Gt

forms over other conformations. Such arguments, however, cannot be applied to explain the cis stability of the ethynylmethyl cyclopropane and the cyanomethyl cyclopropane molecules, because the triple bond electron-rich moiety is expected to repel the ring pseudo-π electrons. Dakkouri and Typke[32] proposed for ethynylmethyl cyclopropane the attractive interaction between the protonated hydrogen of the ethynyl group, and the surface orbitals of the ring are substantially responsible for the prefererability of the cis conformer. Such argument cannot be used to explain the cis stability of cyanomethyl cyclopropane. Also, due to the large distance between the acetylene hydrogen and the three-membered ring, the hydrogen-bonding described by Dakkouri and Typke[32] is too weak to be the major factor contributing to the cis stability.

Dakkouri and Typke[32] also proposed that the dominating factor determining the amount of cis conformer present at ambient temperature be the electronegativity of the substitutent on the methylene group. For ethynylmethyl cyclopropane where the ethynyl group has an electronegativity[33] of 3.1, there is 48 ± 2% of the cis form present[11] at ambient temperature. However, when the substitutent is the Cl atom with a similar electronegativity of 3.0, there is only 12 ± 1% of the cis form present[8] at ambient temperature. For aminomethyl cyclopropane where the amino group has an electronegativity[33] of 2.99, almost the same as Cl, there is only 9% of the cis form present. Therefore, factors other than the electronegativity of the substituent are probably more important in controlling the abundance of the cis form. The conformational stability of fluoromethyl cyclopropane (F with an electronegativity of 4.0) would be of interest for comparison with this series and by using low-temperature rare gas solution it should be possible to obtain these data.

Acknowledgment. J. R. D. acknowledges the University of Missouri − Kansas City for a Faculty Research grant for partial financial support of this research. W. A. H. and B. J. V. thank the FWO-Vlaanderen for their assistance toward the purchase of spectroscopic equipment used in this study. The authors thank the Flemish Community for financial support through the Special Research Fund (BOF) and the Scientific Affairs Division of NATO for travel funds between our two laboratories.

Supporting Information Available: Table 1S, listing symmetry coordinates for aminomethyl cyclopropane; Table 2S, listing structural parameters, rotational constants and dipole moments for the *Cg*, *Gg-2* and *Ct* rotamers of aminomethyl cyclopropane; and Table 3S, listing calculated diagonal force constants of the five conformations of aminomethyl cyclopropane. This material is available free of charge via the Internet at http://pubs.acs.org.

References and Notes

(1) Scott, R. A.; Scheraga, H. A. *J. Chem. Phys.* **1966**, *45*, 2091.
(2) Fujiwara, F. G.; Chang, J. C.; Kim, H. *J. Mol. Spectrosc.* **1977**, *41*, 177.
(3) Mohammadi, M. A.; Brooks, W. V. F. *J. Mol. Spectrosc.* **1978**, *73*, 347.
(4) Mohammadi, M. A.; Brooks, W. V. F. *Can. J. Spectrosc.* **1978**, *23*, 181.
(5) Schei, S. H. *Acta Chem. Scand. Ser. A* **1983**, *37*, 15.
(6) Kalasinsky, V. F.; Wurrey, C. J. *J. Raman Spectrosc.* **1980**, *9*, 315.
(7) Wurrey, C. J.; Krishnamoorthi, R.; Pechsiri, S.; Kalasinsky, V. F. *J. Raman Spectrosc.* **1982**, *12*, 95.
(8) Durig, J. R.; Shen, S.; Zhu, X.; Wurrey, C. J. *J. Mol. Struct.* **1999**, *485*−*486*, 501.
(9) Stolevik, R.; Bakken, P. *J. Mol. Struct.* **1989**, *196*, 285.
(10) Saebo, S.; Kavana, K. *J. Mol. Struct.* **1991**, *235*, 447.
(11) Guirgis, G. A.; Wurrey, C. J.; Yu, Z.; Zhu, X.; Durig, J. R. *J. Phys. Chem. A* **1999**, *103*, 1509.
(12) Dakkouri, M.; Typke, V. *J. Mol. Struct.* **2000**, *550*−*551*, 349.
(13) Wurrey, C. J.; Shen, S.; Zhu, X.; Zhen, H.; Durig, J. R. *J. Mol. Struct.* **1998**, *449*, 203.
(14) Durig, J. R.; Zheng, C.; Herrebout, W. A.; Gounev, T.; van der Veken, B. J. submitted to *J. Phys. Chem.*
(15) Galabov, B.; Kenny, J. P.; Schaefer, H. F.; Durig, J. R. *J. Phys. Chem. A* **2002**, *106*, 3625.
(16) Frisch, M. J.; Trucks, G. W.; Schlegel, H. B.; Scuseria, G. E.; Robb, M. A.; Cheeseman, J. R.; Zakrzewski, V. G.; Montgomery, J. A., Jr.; Stratmann, R. E.; Burant, J. C.; Dapprich, S.; Millam, J. M.; Daniels, A. D.; Kudin, K. N.; Strain, M. C.; Farkas, O.; Tomasi, J.; Barone, V.; Cossi, M.; Cammi, R.; Mennucci, B.; Pomelli, C.; Adamo, C.; Clifford, S.; Ochterski, J.; Petersson, G. A.; Ayala, P. Y.; Cui, Q.; Morokuma, K.; Malick, D. K.; Rabuck, A. D.; Raghavachari, K.; Foresman, J. B.; Cioslowski, J.; Ortiz, J. V.; Stefanov, B. B.; Liu, G.; Liashenko, A.; Piskorz, P.; Komaromi, I.; Gomperts, R.; Martin, R. L.; Fox, D. J.; Keith, T.; Al-Laham, M. A.; Peng, C. Y.; Nanayakkara, A.; Gonzalez, C.; Challacombe, M.; Gill, P. M. W.; Johnson, B. G.; Chen, W.; Wong, M. W.; Andres, J. L.; Head-Gordon, M.; Replogle, E. S.; Pople, J. A. *Gaussian 98*, revision A.11.2; Gaussian, Inc.: Pittsburgh, PA, 1998.
(17) Møller, C.; Plesset, M. S. *Phys. Rev.* **1934**, *46*, 618.
(18) Marstokk, K. M.; Møllendal, H. *Acta Chem. Scand. A* **1984**, *38*, 387.
(19) Pulay, P. *Mol. Phys.* **1969**, *17*, 197.
(20) Guirgis, G. A.; Hsu, Y. D.; Vlaservich, A. C.; Stidham, H. D.; Durig, J. R. *J. Mol. Struct.* **1996**, *378*, 83.
(21) Frisch, M. J.; Yamaguchi, Y.; Gaw, J. F.; Schaefer, H. F., III; Binkley, J. S. *J. Chem. Phys.* **1986**, *84*, 531.
(22) Amos, R. D. *Chem. Phys. Lett.* **1986**, *124*, 376.
(23) Polavarapu, P. L. *J. Phys. Chem.* **1990**, *94*, 8106.
(24) Chantry, G. W. In *The Raman Effect*, Vol. 1, Chapter 2; Anderson, A., Ed.; Marcel, Dekker Inc.: New York, 1971.
(25) Wurrey, C. J.; Nease, A. B. In *Vibrational Spectra and Structure*, Vol. 7, Chapter 1; Durig, J. R., Ed.; Elsevier Science Publishing Company Inc.: New York, 1978.
(26) Durig, J. R.; Zheng, C. *Struct. Chem.* **2001**, *12*, 137.
(27) van der Veken, B. J.; Herrebout, W. A.; Durig, D. T.; Zhao, W.; Durig, J. R. *J. Phys. Chem. A* **1999**, *103*, 1976.
(28) McKean, D. C. *J. Mol. Struct.* **1984**, *113*, 251.
(29) Durig, J. R.; Ng, K. W.; Zheng, C.; Shen, S. *Struct. Chem.* **2003**, in press.
(30) Wollrab, J. E.; Laurie, V. W. *J. Chem. Phys.* **1968**, *48*, 5058.
(31) Herrebout, W. A.; Zheng, C.; van der Veken, B. J.; Durig, J. R. *J. Mol. Struct.* **2003**, *645*, 109.
(32) Caminati, W.; Danieli, R.; Dakkouri, M.; Bitschenauer, R. *J. Phys. Chem.* **1995**, *99*, 1867.
(33) Inamoto, N.; Masuda, S. *Chem. Lett.* **1982**, 1003.